Science of the Total Environment 918 (2024) 170550

Contents lists available at ScienceDirect

Science of the Total Environment

journal homepage: www.elsevier.com/locate/scitotenv

Monthly average air pollution models using geographically weighted regression in Europe from 2000 to 2019

Youchen Shen [a,*], Kees de Hoogh [a,b,c], Oliver Schmitz [d], Nick Clinton [e], Karin Tuxen-Bettman [e], Jørgen Brandt [f], Jesper H. Christensen [f], Lise M. Frohn [f], Camilla Geels [f], Derek Karssenberg [d], Roel Vermeulen [a,g], Gerard Hoek [a]

[a] Institute for Risk Assessment Sciences, Utrecht University, Utrecht, the Netherlands
[b] Swiss Tropical and Public Health Institute, Basel, Switzerland
[c] University of Basel, Basel, Switzerland
[d] Department of Physical Geography, Faculty of Geosciences, Utrecht University, Utrecht, the Netherlands
[e] Google, Inc, Mountain View, California, United States
[f] Department of Environmental Science, Aarhus University, Roskilde, Denmark
[g] Julius Centre for Health Sciences and Primary Care, University Medical Centre, Utrecht University, Utrecht, the Netherlands

HIGHLIGHTS

- We developed monthly Europe-wide LUR models in 20 years for NO_2, O_3, PM_{10} and $PM_{2.5}$.
- Our monthly LUR model estimates are at 25 m spatial resolution.
- Monthly variations were observed in model structures and estimated concentrations.
- Monthly LUR models improved prediction compared to monthly adjusted annual estimates.
- Our estimates will facilitate studies on intermediate-term health effects of air pollution.

GRAPHICAL ABSTRACT

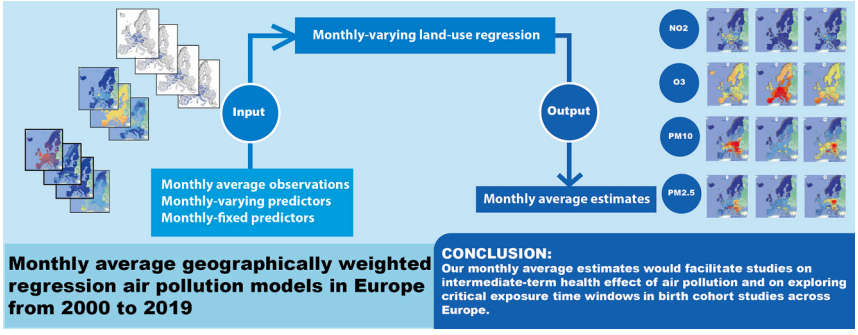

ARTICLE INFO

Editor: Hai Guo

Keywords:
Air pollution
Land-use regression
Monthly variation
Europe-wide
Spatiotemporal variation

ABSTRACT

Detailed spatial models of monthly air pollution levels at a very fine spatial resolution (25 m) can help facilitate studies to explore critical time-windows of exposure at intermediate term. Seasonal changes in air pollution may affect both levels and spatial patterns of air pollution across Europe.

We built Europe-wide land-use regression (LUR) models to estimate monthly concentrations of regulated air pollutants (NO_2, O_3, PM_{10} and $PM_{2.5}$) between 2000 and 2019. Monthly average concentrations were collected from routine monitoring stations. Including both monthly-fixed and -varying spatial variables, we used supervised linear regression (SLR) to select predictors and geographically weighted regression (GWR) to estimate spatially-varying regression coefficients for each month.

Model performance was assessed with 5-fold cross-validation (CV). We also compared the performance of the monthly LUR models with monthly adjusted concentrations.

* Corresponding author.
E-mail address: y.shen@uu.nl (Y. Shen).

https://doi.org/10.1016/j.scitotenv.2024.170550
Received 19 October 2023; Received in revised form 2 January 2024; Accepted 27 January 2024
Available online 4 February 2024
0048-9697/© 2024 The Authors. Published by Elsevier B.V. This is an open access article under the CC BY license (http://creativecommons.org/licenses/by/4.0/).

Results revealed significant monthly variations in both estimates and model structure, particularly for O_3, PM_{10}, and $PM_{2.5}$. The 5-fold CV showed generally good performance of the monthly GWR models across months and years (5-fold CV R^2: 0.31–0.66 for NO_2, 0.4–0.79 for O_3, 0.4–0.78 for PM_{10}, 0.46–0.87 for $PM_{2.5}$). Monthly GWR models slightly outperformed monthly-adjusted models. Correlations between monthly GWR model were generally moderate to high (Pearson correlation >0.6).

In conclusion, we are the first to develop robust monthly LUR models for air pollution in Europe. These monthly LUR models, at a 25 m spatial resolution, enhance epidemiologists to better characterize Europe-wide intermediate-term health effects related to air pollution, facilitating investigations into critical exposure time windows in birth cohort studies.

1. Introduction

Epidemiological studies have increasingly evaluated health effects related to long-term exposure to outdoor air pollution in multi-country cohort studies across Europe (Bauwelinck et al., 2022; Beelen et al., 2014; Chen et al., 2021; Rodopoulou et al., 2022; Strak et al., 2021; Wolf et al., 2021) or nation-wide studies in large countries like US and Canada (Bowe et al., 2018; Cakmak et al., 2018, 2016; Di et al., 2017; Pappin et al., 2019; Pinault et al., 2017; Weichenthal et al., 2017).

In these studies, long-term exposure to key pollutants has been characterized as annual average concentrations. Annual average concentrations at fine spatial resolution (<1 km) have been sufficient to study the relationship between long-term air pollution exposure and health outcomes, including but not limited to mortality, cardiometabolic morbidity, and cancer in multi-country cohort studies across Europe (Bauwelinck et al., 2022; Chen et al., 2021; Rodopoulou et al., 2022; Strak et al., 2021; Wolf et al., 2021).

However, certain epidemiological studies require a more detailed examination of air pollution's health effects within sensitive time windows, which may require the use of monthly or seasonal average exposure estimates (Gondalia et al., 2021; Jiang et al., 2021; Mortimer et al., 2008; Sun et al., 2022a). For example, birth cohort studies would require air pollution exposure specific to the pregnancy trimester during gestation (Iñiguez et al., 2012; Iñiguez et al., 2016; Pedersen et al., 2013, 2016; Rich et al., 2015). In addition, there are studies that extend their investigation beyond long-term exposures, assessing prior monthly exposures to explore physiological outcomes such as obesity and cardiometabolic health (Fouladi et al., 2020; Kim et al., 2019b; Power et al., 2015). Thus, epidemiologists often require monthly or seasonal average exposure estimates at fine spatial resolution (≤1 km) in order to study intermediate-term health effects of air pollution.

Monthly average air pollution concentrations are currently estimated using various methods. Firstly, deterministic air pollution atmospheric models provide spatiotemporal variations in air pollution. These variations are calculated based on input data such as meteorological, terrain information, and detailed emission data. In Europe, such input data and estimates are available at a 20 km resolution (Brandt et al., 2012), while in Scandinavia, they are available at a finer 1 km resolution (Frohn et al., 2022). However, this finer spatial resolution is unapplicable across larger geographical extents. Secondly, in some epidemiological studies, monthly average residential exposures are derived by spatially interpolating monthly average observations from nearby monitoring stations (Fouladi et al., 2020; Kim et al., 2019a; Patterson et al., 2021). In specific cases, residential exposures are characterized by spatially-interpolated regional background concentrations, supplemented with near-road concentrations estimated by the dispersion model CALINE-4 in the Californian study (Kim et al., 2019a). However, this spatial interpolation method is constrained by the availability of the nearby regional background observations and the implementation of the dispersion model. Thirdly, other epidemiological studies use temporal adjustment approach to refine estimates from annual land-use regression (LUR) models, based on daily or monthly observations from a few nearby background monitoring stations (Bechle et al., 2015; Iñiguez et al., 2016; Pedersen et al., 2013; Slama et al., 2007). This approach relies on the annual LUR model estimates to reflect spatial patterns of air pollution, with the assumption that the spatial patterns remain stable across months through temporal adjustments. The assumption is rooted in the high temporal correlation often observed in measurements from nearby sites (Ito et al., 2005). However, this approach may overlook spatial variations that exhibit month-to-month differences arising from specific local sources (Hoek, 2017; Jerrett et al., 2005), highlighting the benefit to incorporate interannual (seasonal and monthly) variations in exposure assessment (Beckerman et al., 2013; Lu et al., 2020; Yanosky et al., 2008). Consequently, the assessment of air pollution exposure can be improved by considering the spatio-temporal variations resulting from monthly and seasonal dynamics of human activity, meteorological conditions, and emission sources (Hannam et al., 2013).

Due to these dynamics, air pollution concentrations exhibit monthly and seasonal variations in the spatial patterns (Almeida et al., 2020; Barmpadimos et al., 2011, 2012; Duncan and Bey, 2004; Guevara et al., 2021; Juda-Rezler et al., 2020; Morawska et al., 2021; Ordónez et al., 2005; Tan et al., 2023; Ye et al., 2018). For example, both southeastern and southwestern Europe experience warmer summers than northwestern Europe, while winter temperatures are lower in the southeastern and higher in the southwestern compared to northwestern Europe. These changing atmospheric, meteorological, and emission patterns can be integrated into monthly-varying LUR models. Such models are designed to capture the monthly variations in air pollution concentrations, thereby improving the predictions in the concentrations.

Monthly LUR models have been built separately per month, incorporating monthly-varying spatial predictors, mainly meteorology, satellite retrievals, and chemical transport model (CTM) estimates in previous studies. Studies conducted outside of Europe have demonstrated that monthly LUR models can capture monthly variations at national and continental scales (Araki et al., 2020; Beckerman et al., 2013; Knibbs et al., 2014; Lu et al., 2021; Yanosky et al., 2008; Zhang et al., 2018).

A handful of studies have endeavoured to develop monthly LUR models over extended time periods, such as those in Bern, Switzerland (Proietti et al., 2016) or at a global scale with a coarse spatial resolution (equal to or coarser than 1 km) (Sun et al., 2022b; Van Donkelaar et al., 2021). Alternatively, one could derive monthly estimates by aggregating daily LUR model estimates. However, it is essential to acknowledge that the development of daily LUR models at a fine spatial resolution (<100 m) requires a different methodology compared to the one used in this study and is currently unfeasible to be achieved due to practical constraints in terms of both time and computational resources. Therefore, our focus is directed towards the development of individual monthly LUR models for each month across Europe.

Our primary motivation for developing monthly LUR models is the benefit for estimating monthly average exposures at a finer spatial resolution than currently achievable with deterministic air pollution atmospheric models or daily LUR models. However, we posit that in scenarios with changing spatial patterns across months, the performance of high-resolution annual models could be enhanced by developing monthly models and subsequently aggregating the monthly average estimates into annual averages. This endeavour builds upon our previous Europe-wide models of annual average concentrations at a

resolution of 25 m (Shen et al., 2022).

Our main research goal is to evaluate the performance of Europe-wide LUR models at a high spatial resolution (25 m) for each month from 2000 to 2019, including four key pollutants: nitrogen dioxide (NO_2), ozone (O_3), particulate matter <10 μm (PM_{10}), and particulate matter <2.5 μm ($PM_{2.5}$). Our second goal involves comparison between monthly concentrations estimated by our monthly LUR models and those derived from monthly-adjusted LUR models. Finally, our third goal is to assess the significance of capturing monthly variations in air pollution concentrations to enhance the exposure assessment of annual average air pollution.

2. Materials and methods

We extended our previous Europe-wide annual LUR models at a monthly scale (de Hoogh et al., 2018a; Shen et al., 2022). Geographically weighted regression (GWR) was used to capture the spatial variations in monthly air pollution concentrations for each month from 2000 to 2019 for NO_2, O_3, and PM_{10} and from 2006 to 2019 for $PM_{2.5}$.

Observations of ambient air pollution from routine monitoring stations were collected for four pollutants and averaged every month. Using both monthly-fixed and -varying spatial predictor variables, we developed monthly LUR models at a 25 m resolution. To assess the model performance, we implemented 5-fold cross-validation (CV). Furthermore, we compared estimates from our monthly LUR model with estimates adjusted monthly from our annual LUR estimates (denoted as YRADJ_LUR). This adjustment was done using inverse distance weighting (IDW) interpolation of monthly average observations.

The local spatial variations, especially contributed by traffic emission sources, can be large for NO_2, O_3 and $PM_{2.5}$. To capture near-roadway variations in air pollution concentrations, we develop monthly LUR models at a notably high spatial resolution (25 m). Moreover, to illustrate the benefit of 25 m spatial resolution, we compare predictions at different spatial resolutions (25 m, 100 m, 1 km).

2.1. Routine-monitoring observations

We collected routine monitoring observations for NO_2, O_3, PM_{10}, and $PM_{2.5}$ from the European Environmental Agency (EEA). Our processing method aligned with the details in our preceding study (Shen et al., 2022). In brief, we calculated monthly averages for stations where >75 % of daily or hourly observations within each month were valid according to EEA-defined criteria. For PM_{10} and $PM_{2.5.}$, we aggregated daily observations into monthly. For NO_2, we aggregated hourly observations into monthly. For O_3, we calculated the daily maximum 8-h mean per day from hourly data and aggregated the values into monthly, according to health-related air quality guidelines (WHO, 2021). The number of valid monthly average observations across Europe for each pollutant, month, and year can be found in Tables A1-A4. The stations are categorized as background, industrial, or traffic stations by the EEA, depending on the presence of dominant nearby emission sources (European Environment Agency, 2021).

2.2. Predictor variables

We incorporated a range of potential predictors, including those related to road traffic, land use, meteorology, satellite retrievals, and chemical transport model (CTM) estimates, as detailed in Table A5. The predictors used in this study were similar to those in our previous study (Shen et al., 2022), with the addition of some monthly-varying variables in this study. These variables include meteorological variables and some satellite retrievals (such as OMI) and CTM estimates such as MACC model (Marécal et al., 2015) for NO_2 and $PM_{2.5}$ in 2010, and the Danish Eulerian Hemispheric Model (DEHM) (Brandt et al., 2012) for all pollutants in every year. Other satellite retrievals were annually-varying. Spatial land-use variables were either temporally-fixed (i.e., altitude and population) or updated every 3 or 6 years (i.e., CORINE land use and impervious density). Road-related predictors remained temporally constant and were obtained from OpenStreetMap, a crowd-sourced database. These road predictor variables were available at 25 m resolution, while land-use data at 100 m resolution, and satellite retrievals and CTM estimates were available at a resolution of 1 km × 1 km or coarser.

2.3. Monthly LUR using geographically weighted regression (GWR)

GWR is a linear regression that uses spatially-varying coefficient values (Brunsdon et al., 1996). It uses a kernel function to give weights to observation points as a function decaying by distance to regression points (i.e., the closer the observation is to a regression point in space, the higher weight the observation has for estimating the regression coefficients for that regression point).

As shown in our previous study of annual modelling (Shen et al., 2022), GWR explained spatial variations in ground-based observations better than supervised linear regression (SLR) and random forests (RF), and one single model performed similarly or slightly worse than individual annual models. In our preliminary test for monthly modelling (shown in Supplementary Material's section 1&2), we found that GWR and RF performed similarly better than SLR based on 5-fold cross-validation (CV). Moreover, we found that one single monthly model performed worse than individual monthly models. Therefore, we developed individual monthly GWR models to estimate the ambient monthly air pollution concentrations, because GWR offers a more interpretable model compared to RF.

In GWR, we had spatially-varying linear regression coefficient values of predictors selected by SLR, following the same procedure used in our previous studies (Chen et al., 2021; de Hoogh et al., 2018a; Eeftens et al., 2012; Shen et al., 2022).

In SLR, firstly we built a univariate linear regression with one predictor variable that had the highest adjusted coefficient of determination (adjusted R^2) in air pollution observations and that had the statistically-significant coefficient value ($P < 0.1$), if the coefficient value matched the plausible direction of effect (as defined in Table A5). Then in each step we added one of the remaining variables that meet our above-mentioned criteria. After no additional variable would meet our criteria, we excluded variables with variance inflation factor larger than 3 to avoid multicollinearity in our final linear regression model.

Then we used GWR to estimate the spatially-varying regression coefficient values of the predictors selected by SLR. The regression coefficients were at 200 km × 200 km spatial resolution. We used an exponential function as our decay function, and the bandwidth (i.e., how fast the kernel function decays to zero) was determined by CV within the training data. Details can be found in our previous study (Shen et al., 2022). The calculation was done in R using the *GWmodel* package version 2.2–4 (Gollini et al., 2015; Lu et al., 2014; R Core Team, 2020). We built a monthly LUR model from 2000 to 2019 for every calendar month in which the total number of monthly averaged observations was >200 sites across Europe. This meant that we were only able to build monthly $PM_{2.5}$ models after 2006 and from 2000 to 2019 for the other pollutants (Tables A1-A4).

2.4. Evaluate model performance: 5-fold cross-validation (CV)

We used 5-fold CV to evaluate the accuracy of our monthly LUR model estimates. We created each fold randomly. We ensured the observation points had similar proportion of different station characteristic across the whole dataset, training dataset and validation dataset. The station characteristic includes climate zones (i.e., Alpine, Atlantic, Continental, Northern, Southern, as shown in Fig. A2) and routine monitoring station types (i.e., background, industrial, traffic, as provided by EEA). The hold-out data from all 5 folds were combined to obtain one value of each performance metric.

In the 5-fold CV analysis, we used three performance metrics: mean-square-error-based R^2 (MSE-R^2), root mean square error (RMSE), and relative RMSE (rRMSE) defined as Eqs. 1, 2 & 3. The MSE-R^2 reflects the systematic bias and random difference between model estimates and observations along the 1:1 line. In contrast, the RMSE measures the absolute average difference between estimates and observations with extra weight added to larger estimate errors, and the rRMSE gives a normalized measure of RMSE to mitigate variabilities in air pollution levels across months.

$$MSE-R^2 = 1 - \frac{\sum_{i=1}^{N}(y_i - \hat{y}_i)^2}{\sum_{i=1}^{N}(y_i - \bar{y})^2} \quad (1)$$

$$RMSE = \sqrt{\frac{1}{N}\sum_{i=1}^{N}(y_i - \hat{y}_i)^2} \quad (2)$$

$$rRMSE = \frac{RMSE}{\bar{y}} \quad (3)$$

where y_i is the observed monthly average concentration at station i, $\hat{y}_i$ is the estimated monthly average concentrations at station i, and $\bar{y}$ is the average observations from all N stations.

To compare accuracy of our monthly LUR with YRADJ-LUR models, we used the monthly background observations from the same training set as the monthly LUR models in each fold to obtain IDW_i for month i (Eqs. 1 & 2). Although the training data of annual LUR model ($LUR_{yr=2010}$ in Eqs. 1 & 2) included annual averages of observations from the monthly validation set, we assume that $LUR_{yr=2010}$ contains no information of monthly air pollution spatial patterns anymore after aggregation.

To compare accuracy of estimated annual averages from our monthly LUR models with our previous annual LUR model estimates, we aggregated our hold-out monthly observations into annual average estimates with the 75 % validity criterion (i.e., >9 monthly observations available at a monitoring site in a year). Then we calculated the model performance metrics for the hold-out annual observations at stations where both monthly observations and annual observations were available.

2.5. Monthly-adjusted estimates of annual LUR model (YRADJ-LUR)

We built and evaluated the monthly performance of annual LUR adjusted by monthly averaged monitoring data (Basso et al., 1999). We used this approach to evaluate the potential gain in performance obtained by the monthly LUR models for a single year. We implemented this approach for only the year 2010, which is the midpoint of our study period and the starting point of our previous studies (Chen et al., 2019; de Hoogh et al., 2018a). For each month, we adjusted our annual average estimates obtained from the geographically and temporally weighted regression (GTWR) models built in our previous study (Shen et al., 2022). We refer to these monthly adjusted estimates as YRADJ-LUR. We compared the YRADJ-LUR estimates with our monthly LUR estimates.

To adjust annual averaged estimates to monthly averaged estimates, we first spatially interpolated monthly background observations using IDW. Although IDW is a relatively simple approach to aggregate nearby monitoring data, it is sufficient and has been applied in previous studies, because of the high correlation of the air pollution observations at nearby stations over time and space (Ito et al., 2005). We used *inverse-Distance* function in Google Earth Engine (GEE) (Gorelick et al., 2017) to interpolate the background observations. We set the interpolation range as 70 km and the decay factor gamma as 1 (Eckel et al., 2016; Wong et al., 2004). When no monthly background observation point was within 70 km, we set the interpolated values as the monthly average background concentration across Europe (Kim et al., 2019a; Wong et al., 2004). Background observations were collected at stations where air pollution is not dominated by nearby emission sources and where pollution concentrations represent average exposure of the population, as defined by the EEA. Background stations were in both rural and urban areas.

For year 2010, with the monthly interpolated values (IDW_i) for month i, we monthly adjusted the annual LUR estimates ($LUR_{yr=2010}$) into monthly estimates ($YRADJ\text{-}LUR_i$) using either the differencing method (Eq. 4) or the ratio method (Eq. 5) (Gulliver et al., 2013):

$$\mathrm{YRADJ^{-}LUR_i} = \mathrm{LUR_{yr=2010}} + \mathrm{IDW_i} - \frac{\left(\sum_{j=1}^{12}\mathrm{IDW_j}\right)}{12} \quad (4)$$

$$\mathrm{YRADJ^{-}LUR_i} = \mathrm{LUR_{yr=2010}} \times \frac{\mathrm{IDW_i}}{\left(\sum_{j=1}^{12}\mathrm{IDW_j}\right)\Big/12} \quad (5)$$

We refer to YRADJ-LUR estimates obtained by Eq. 4 as '*diff*' and estimates obtained by Eq. 5 as '*ratio*'.

We evaluated the model accuracy of the YRADJ-LUR using 5-fold CV with the same setup of training and test folds described in Section 2.4. We then compared 5-fold CV of the two approaches (YRADJ-LUR and monthly LUR).

We also calculated the Pearson correlation coefficient of the estimates from the two approaches at around 77 thousand random points in populated regions. The points were created at the impervious and populated areas, defined as IMD > 0 in the impervious data (Copernicus, 2021) and pop>0 in the population data from year 2011 (see Table A5). The number of the random points is proportional to the population in each NUTS1 region (Nomenclature of territorial units for statistics) in year 2021 (EUROSTAT, 2021), and at least 300 points were created in each NUTS1 region (Fig. A1). The NUTS1, defined by Eurostat, represents the major socio-economic regions in Europe. These random points were used to represent the residential addresses.

2.6. Comparison of air pollution predictions at different spatial scales (25 m, 100 m, 1 km)

Previous monitoring studies have shown large near-roadway gradients of traffic-related pollutants, including NO_2, black carbon (BC), and ultrafine particles (UFP) within the first tens of meters from the nearby road (HEI, 2022; Niepsch et al., 2022; Zhu et al., 2002). Thus, to illustrate the benefit of estimating air pollution at very fine spatial scales, we compared air pollution predictions at different spatial scales, namely at 25 m, 100 m, and 1 km. For the comparison, we extracted predicted values at the 77 thousand random points mentioned in Section 2.5 for calculating the Pearson's correlation. Moreover, to examine local near-roadway differences, we extracted predicted values along a transect for a major city (Paris).

3. Results and discussion

Fig. A3 and A4 show variabilities in monthly average air pollution levels, as observed at ground-based monitoring sites for four pollutants during selected years (i.e., year 2000, 2005, 2010, 2015, and 2019). The figures reveal findings on seasonal patterns and spatial heterogeneity in air pollution levels and distributions.

Across all selected years, consistent seasonal patterns were observed. Higher O_3 levels were shown in the summer months. In contrast, lower NO_2 and PM levels were observed in the summer months.

Beyond monthly variabilities, distribution patterns also exhibited substantial spatial heterogeneity across months. The large-scale monthly distribution patterns were reflected by the monthly averages of all observations per climatic region, per month and per year, as documented in Fig. A4.

The evident variabilities, particularly for O_3 and PM, emphasized the need to build individual monthly LUR models per month and per year. This approach is essential for capturing the dynamic characteristics of the air pollution levels and patterns.

For NO_2, O_3, and PM_{10}, the monthly LUR models were built and evaluated for every month from 2000 to 2019. For $PM_{2.5}$, due to the availability of ground-based observations, we only built and evaluated monthly models for every month from 2006 to 2019.

In Section 3.1, we present and discuss the predictors selected and used in our monthly LUR models. In Section 3.2, we document the model performance of our monthly LUR models and compare the monthly LUR with the annual LUR and YRADJ-LUR. In Section 3.3, we examine the monthly variations in our monthly LUR estimates. In Section 3.4, we compare predictions at different spatial resolution (25 m, 100 m, 1 km) and discuss the benefit of fine-scale predictions. Finally in Section 3.5, we discuss limitations of our study.

3.1. Monthly LUR model structure

Fig. 1 and Fig. A5 document the predictor variables selected and used in the monthly LUR models per pollutant per season (or per month) thorough the study period (2000–2019 for NO_2, O_3 and PM_{10}; 2006–2019 for $PM_{2.5}$). Overall, very few variables were selected in almost all months with some variables selected in only specific months. The selection of the predictor variables reflects factors to which the monthly air pollution levels can be attributed. The degree of the contribution from individual variables selected can be represented by the regression slope (in $\mu g/m^3$), as documented in Fig. A6. The contribution of some selected variables exhibited great monthly variabilities, indicating the dynamic patterns of air pollution driven by the seasonally and monthly variabilities in emission activities and dispersion processes. We continue the discussion of the predictors that vary per month for each pollutant as follows.

For NO_2, the variables selected most frequently across months and years were near-roadway variables (with 50 m–100 m buffer size), wind speed, population, CTM predictor (MACC model) (Fig. 1). OMI satellite data were selected more frequently in cold seasons than in warm seasons, while temperature showed the opposite trend. MACC model variable contributed the most (with highest slope) to explaining monthly variations in air pollution (Fig. A6 1-F), followed by near-roadway variables (Fig. A6 1-A & A6 1-C) with stable monthly contribution. The same result was also observed in our previous Europe-wide study of building annual LUR (de Hoogh et al., 2018a), and we further showed that the contribution of MACC was higher in cold seasons than in warm seasons. This could be because MACC performed better in winter than in summer (Pearson's cor = 0.31 in winter and 0.15 in summer) at 285 ground-based rural stations (Giordano et al., 2015). All in all, we found the spatial patterns of NO_2 monthly concentrations were mainly influenced by not only near-roadway traffic emission sources, but also meteorological conditions (wind speed and temperature) and regional background concentrations presented by satellite retrievals (OMI) and CTM estimates (MACC).

For O_3, altitude and temperature were selected most frequently across months and years (Fig. 1). Population and DEHM were selected

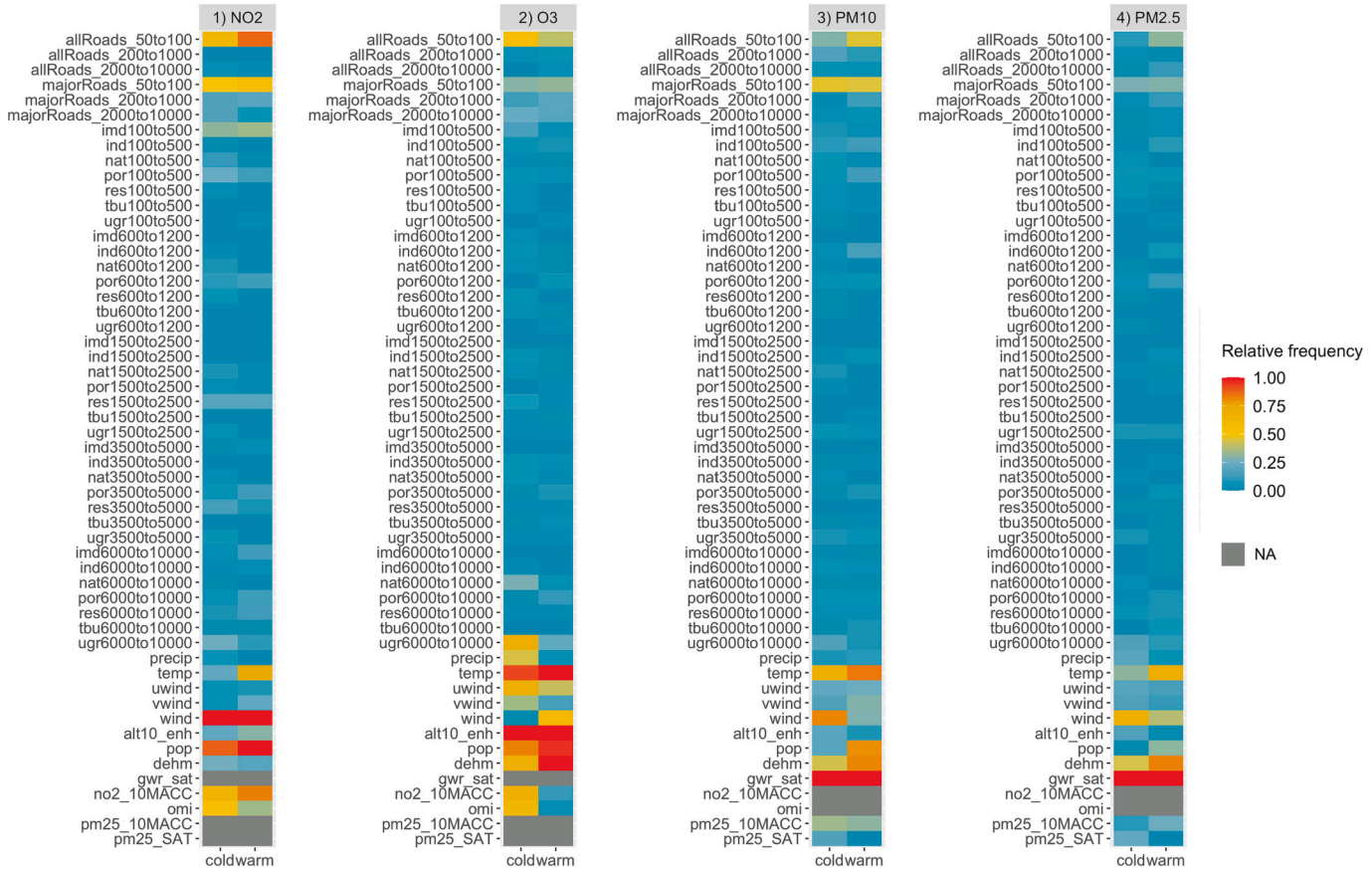

Fig. 1. Variables selected by SLR and the used in GWR for cold seasons (Jan-Mar and Oct-Dec) and warm seasons (Apr-Sept) from 2000 to 2019 for 1) NO_2, 2) O_3, 3) PM_{10} and from 2006 to 2019 for 4) $PM_{2.5}$. Fill colour indicates relative frequency of a variable being selected over the 20-year or 14-year period per season. Different columns indicate seasons (warm and cold). Different rows indicate variables shown as variable code (defined in Table A5). To reduce complexity of visualization, variables with similar buffer sizes in same categories are combined: allRoads and majorRoads with groupings of 50 m–100 m (50to100), 200 m–1000 m (200to1000), 2000 m–10,000 m (2000to10000); imd, ind, nat, por, res, tbu, and ugr with groupings of 100 m–500 m (100to500), 600 m–1200 m (600to1200), 1500 m–2500 m (1500to2500), 3500 m–5000 m (3500to5000), 6000 m–10,000 m (6000to10000). NA: Not applicable (where variables were not potential predictors for a pollutant).

more frequently in warm seasons than in cold seasons, whereas NO_2 MACC and OMI data were selected more frequently in cold seasons. Similar results were also found in the previous Europe-wide study (de Hoogh et al., 2018a) where seasonal O_3 LUR models selected either MACC or DEHM data. In our monthly O_3 LUR models, temperature contributed the most, followed by altitude and DEHM data. These frequently selected variables contributed differently across months (Fig. A6 2-D, A6 2-E & A6 2-F) with higher contribution of population and DEHM in warm seasons than in cold seasons.

The dominant contribution of temperature and altitude represents regional variations of O_3. The regional variations were also represented by population, large-scale urban green (6 km–10 km), MACC (10 km), OMI (13 km × 24 km) and DEHM data (~50 km). On the other hand, the near-roadway variables (Fig. A6 2-A & A6 2-C) in our LUR represent the local near-roadway depletion of O_3 due to photochemical reactions that consume nitrogen oxide (NO) and O_3 to form NO_2 in the near-road microenvironment.

For PM_{10}, the geophysical statistical surface concentration estimates (gwr_sat) were selected in all months and contributed the most with large monthly variations (higher contribution in cold seasons than in warm seasons) (Fig. A6 3-F & A6 4-F), whereas the DEHM data was selected more frequently in warm seasons than in cold seasons and contributed quite consistently across months. These two variables represent different aspects of variations in PM_{10}. The gwr_sat estimates were based on satellite observed aerosol optical depth (AOD) and GEOS-Chem CTM model (Hammer et al., 2020; Van Donkelaar et al., 2019). Thus, the monthly-varying contribution of geophysical statistical estimates could result from either the monthly-varying PM_{coarse} (subtract $PM_{2.5}$ from PM_{10}) or the large monthly or seasonal variability in PM emission patterns, representing the local patterns of $PM_{2.5}$ varying at a few kilometres. On the other hand, the DEHM data represent the large-scale variations of PM_{10} at 50 km resolution, and its contribution was more seasonally and monthly stable compared to the geophysical statistical estimates.

Like the PM_{10} monthly models, $PM_{2.5}$ models also selected the geophysical statistical estimates (gwr_sat) in all months with large monthly-varying contribution. But the $PM_{2.5}$ models selected near-roadway predictors less frequently than the PM_{10} models.

3.2. Model performance

The monthly LUR models performed differently across months, years and air pollutants (as shown in Fig. 2, A7-A9).

For NO_2 (MSE-R^2 = 0.51–0.72; RMSE = 6.2–12.4 μg/m^3, rRMSE = 0.27–0.51), the monthly models' performance remained relatively stable with some variations with lowest performance in summer when the

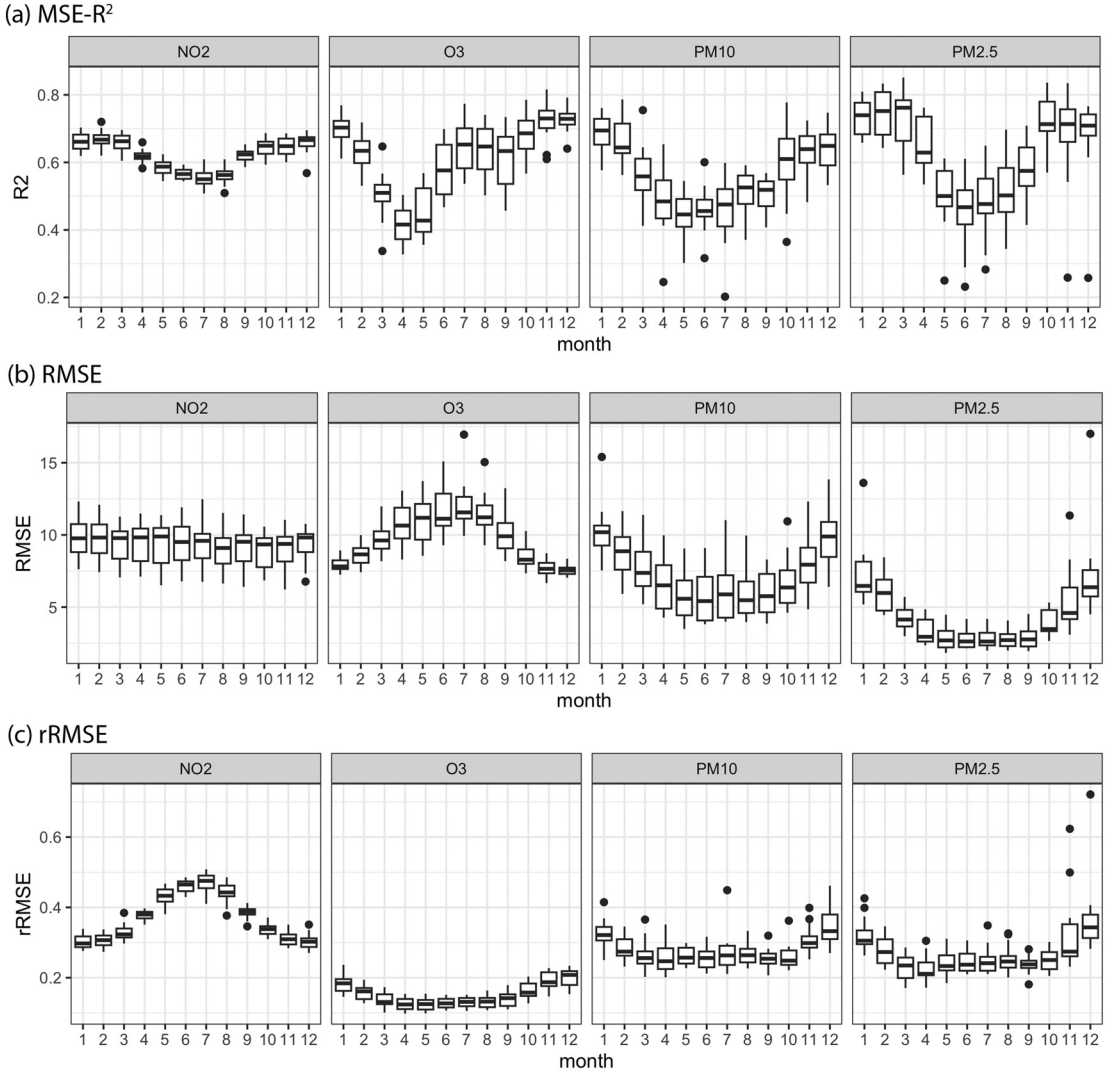

Fig. 2. Boxplots of (a) MSE-R^2, (b) RMSE and (c) relative RMSE values using 5-fold CV per calendar month from 2000 to 2019 for NO_2, O_3, and PM_{10} and from 2006 to 2019 for $PM_{2.5}$. Equations of MSE-R^2, RMSE and relative RMSE are shown in Eqs. 1, 2 & 3.

NO_2 levels are lower.

For O_3 (MSE-R^2 = 0.34–0.82; RMSE = 7–16.9 μg/m^3, rRMSE = 0.1–0.24), MSE-R^2 was lowest in spring. RMSE was highest in summer due to the high O_3 levels. In contrast, after normalizing the variabilities in the levels, rRMSE was lowest in warm season with constant stability across months. The low MSE-R^2 in spring could be primarily driven by the difficulty of the statistical model to capture the variabilities dominated by intrusion of stratospheric ozone with still relatively low photochemical transformation in this season.

For PM_{10} (MSE-R^2 = 0.2–0.78; RMSE = 3.4–15.4 μg/m^3, rRMSE = 0.2–0.46), all performance metrics were lowest in warm seasons. The low MSE-R^2 observed during summer months, especially in the early years (e.g., 2000), can be primarily caused by two factors. Firstly, the relatively small number of observations available impacted the models' abilities to capture air pollution variabilities during the early years. Moreover, the relatively low spatial distribution patterns observed during warm seasons (as depicted in Fig. A4) posed further challenge. Despite these variations and challenges, the overall model performance remained satisfactory based on low rRMSE. It implies low overall difference between observations and estimates, suggesting that the models, while exhibiting some seasonal fluctuations, maintained its overall accuracy in capturing the air pollution levels.

For $PM_{2.5}$ (MSE-R^2 = 0.23–0.85; RMSE = 1.95-17 μg/m^3, rRMSE = 0.17–0.72), like PM_{10}, all performance metrics were also lowest in warm seasons. This observation also aligns with findings from a previous global study (Van Donkelaar et al., 2021), which also documented lower R^2 values during warm seasons compared to cold seasons for year 2018.

It is noteworthy to acknowledge that our study encountered an outlier—a single extreme observation with the $PM_{2.5}$ level above 150 μg/m3 in November and December 2007. This outlier attributed to elevated RMSE values (11.34 and 17 μg/m3) and rRMSE values (0.62 and 0.72) shown in Fig. A8 and A9. However, when considering the overall model performance across various calendar months, we consistently observed moderate to good performance metrics (average MSE-R^2 = 0.55–0.62, RMSE = 4.3–9.7, rRMSE = 0.15–0.37 for the four pollutants).

For O_3, PM_{10}, and $PM_{2.5}$, although the MSE-R^2 and RMSE values were fluctuating across months, the stable rRMSE values demonstrate that the models performed quite well with low prediction errors. The fluctuating MSE-R^2 and RMSE values across months were mainly due to the variability in air pollution levels and distribution patterns observed in Fig. A3 & A4.

3.2.1. *Monthly LUR model estimates vs monthly adjusted annual LUR estimates (YRADJ-LUR)*

3.2.1.1. 5-fold CV of monthly LUR and YRADJ-LUR. The 5-fold CV results show that the monthly LUR estimates gave better accuracy than the YRADJ-LUR estimates using differencing and ratio methods in general (Table 1 & Tables A6 & A7).

For NO_2, the monthly LUR gave slightly higher accuracy than YRADJ-LUR. The differences in accuracy between the methods were small, indicating the spatial patterns were stable across months. This is consistent with the similar spatial patterns shown in our estimated air pollution maps across months in Section 3.3.

For O_3, the monthly LUR had higher accuracy than YRADJ-LUR in all months, and the differences in accuracy between the two were higher in cold season, when the O_3 concentrations were lower, than in warm season.

For PM_{10} and $PM_{2.5}$, the monthly LUR had higher accuracy than YRADJ-LUR in almost all months. The differences in accuracy were higher in warm season, when the PM concentrations were lower, than in cold season. In cold season, the difference in accuracy was small.

Very few studies have compared the model performance between monthly LUR and YRADJ-LUR. We found one study in the United States that monthly adjusted the spatial annual LUR estimates using three

Table 1
5-fold CV MSE-R^2 values of monthly average concentrations estimated by monthly LUR using GWR (column 'gwr') and by YRADJ-LUR using differencing method in Eq. 4 (column 'diff') and ratio method in Eq. 5 (shown in column 'ratio') for each month in the year 2010 for 1) NO_2, 2) O_3, 3) PM_{10}, and 4) $PM_{2.5}$. The highest MSE-R^2 value among the three methods for each month is highlighted in red.

1) NO2

month	gwr	diff	ratio
1	0.63	0.61	0.51
2	0.64	0.64	0.6
3	0.63	0.63	0.6
4	0.62	0.61	0.6
5	0.56	0.57	0.55
6	0.55	0.56	0.53
7	0.53	0.53	0.5
8	0.53	0.52	0.51
9	0.61	0.62	0.61
10	0.61	0.63	0.59
11	0.6	0.6	0.56
12	0.67	0.63	0.51

2) O3

month	gwr	diff	ratio
1	0.74	0.55	0.56
2	0.6	0.51	0.52
3	0.45	0.37	0.34
4	0.38	0.38	0.24
5	0.49	0.49	0.44
6	0.52	0.49	0.4
7	0.71	0.64	0.57
8	0.65	0.6	0.55
9	0.69	0.64	0.64
10	0.75	0.66	0.66
11	0.72	0.57	0.55
12	0.74	0.54	0.52

3) PM10

month	gwr	diff	ratio
1	0.75	0.68	0.69
2	0.69	0.68	0.7
3	0.54	0.54	0.54
4	0.42	0.33	0.34
5	0.45	0.28	0.4
6	0.41	0.29	0.36
7	0.37	0.11	0.17
8	0.58	0.42	0.47
9	0.47	0.37	0.44
10	0.65	0.65	0.64
11	0.67	0.63	0.62
12	0.66	0.65	0.66

4) PM2.5

month	gwr	diff	ratio
1	0.78	0.73	0.79
2	0.75	0.69	0.74
3	0.65	0.71	0.69
4	0.57	0.57	0.57
5	0.53	0.08	0.43
6	0.44	-0.22	0.21
7	0.5	-0.11	0.25
8	0.49	-0.24	0.25
9	0.53	0.17	0.49
10	0.72	0.75	0.75
11	0.6	0.61	0.6
12	0.74	0.64	0.69

spatial interpolation methods (nearest neighbourhood, inverse distance weighting, kriging) for NO_2 over period 2000–2010 (Bechle et al., 2015). The three methods gave similar model performance with kriging explaining 82 %, IDW explaining 79 % and NN explaining 80 % spatial variability. Although they found that the monthly LUR models explained less spatial variability in monthly average observations than the YRADJ-LUR for every month, their monthly LUR models included mostly monthly-fixed spatial variables with only satellite-derived variables being monthly-varying at coarse spatial resolution of 13 km × 24 km at nadir. Since their study, several monthly-varying spatial variables that would contribute to air pollution modelling have become available. These variables were included in our monthly LUR models, including not only satellite-derived variables and chemical transport model estimates at coarse spatial resolutions (13 × 24 km at nadir and 50 km × 50 km) but also meteorological variables at finer spatial resolution (0.1^{o} ~ 12 km). Our satellite data, CTM data and meteorological variables were selected frequently and contributed strongly in our monthly LUR, because these variables helped explaining the spatial variations in the monthly average observations, as shown and discussed in Section 3.1.

Overall, our monthly LUR was better at capturing the spatial variations in the monthly average observations than the monthly adjusted method for NO_2, O_3, PM_{10}, and $PM_{2.5}$, especially in less-polluted months for pollutants with high monthly variations like O_3, PM_{10} and $PM_{2.5}$.

3.2.1.2. Correlations between estimates of monthly LUR and YRADJ-LUR. We compared how predictions of the monthly LUR and YRADJ-LUR models were correlated with one another at 77 random points as shown in Fig. 3. Overall, for NO_2, the correlation between monthly LUR and YRADJ-LUR was high (cor > 0.88) for all months, whereas for O_3 the correlation was moderate to high (cor = 0.64–0.86). For PM, the correlation was high (cor > 0.77) with lower correlation in warm season. Overall, the moderate to high correlation (cor > 0.64) between monthly LUR and YRADJ-LUR estimates suggests that a simple adjustment of annual averages can provide a reasonable approximation of monthly spatial variations, albeit developing specific monthly LUR models are the preferred method.

However, in months where we do not have enough observations to train monthly LUR models, we will still need monthly adjusting approaches to estimate air pollution exposures (before 2006 for $PM_{2.5}$ and before 2000 for the other pollutants). But the monthly adjusting approaches could also be limited by the number of observations and how the stations are spread in space. In our approach, when no background station was available within 70 km, continental (Europe-wide) background averages were used for the temporal adjustment. However, the spatial contrast of the monthly concentrations could be varying across Europe, as shown in Fig. A13. The varying spatial contrast in specific months could explain the low performance of monthly adjusting approaches, because the contrast may not be reflected by the annual LUR estimates adjusted by the continental background averages for locations without background stations available within 70 km.

Other adjusting approaches such as using chemical transport model estimates can overcome this limitation but provide monthly variations at coarse spatial resolution (>10 km). Moreover, the limited $PM_{2.5}$ observations restrain building monthly models before 2006 for $PM_{2.5}$, this problem could be solved by using geographically and temporally weighted regression to estimate monthly air pollution concentrations before 2006.

3.2.2. Monthly LUR model performance vs annual LUR model performance

Overall, the annual averages from our monthly LUR estimates explained slightly more spatial variations in annual average observations than our previous annual LUR estimates from Shen et al. (2022) as shown in Fig. 4. The improvement of annual model performance contributed by developing monthly-varying LURs was minimal for PM_{10}, NO_2 and $PM_{2.5}$ but greater for O_3. On average the increase in MSE-R^2 is 0.017, 0.062, 0.032, and 0.01 and the reduction in RMSE is 0.35, 0.6, 0.32, and 0.1 for NO_2, O_3, PM_{10}, and $PM_{2.5}$ respectively.

The improvement of estimating annual air pollution concentrations could be explained by the within-year variations in predictors and observations contributed in the monthly LUR models. The monthly LUR captured the within-year variations represented by the observations and some predictors (i.e., meteorological, satellite-derived and CTM data) before being aggregated into annual averages, whereas the annual LURs included only the aggregated information of the within-year variations. Another advantage of aggregating the monthly LUR model estimates to annual average concentrations was that the monthly LUR models were trained by more observations from more stations than the annual LUR models due to the 75 % validity criterion of excluding observations from stations with availability <9 months when calculating the annual average observations for training the annual models. The monthly

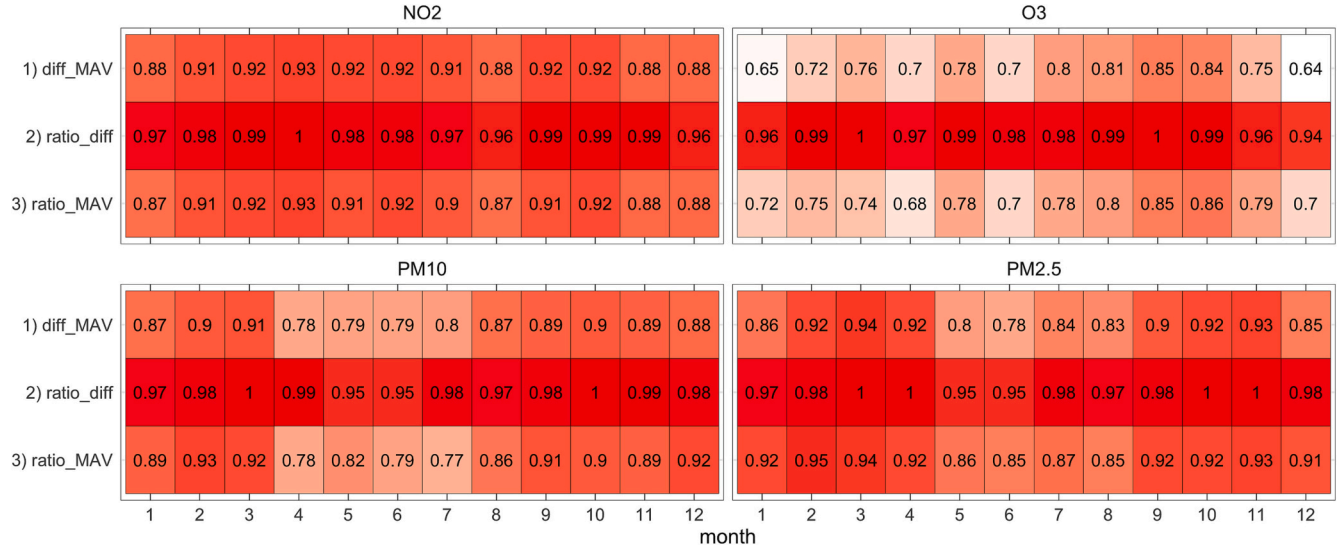

Fig. 3. Correlations between 1) monthly GWR estimates and YRADJ-LUR using differencing method (diff_MAV), 2) YRADJ-LUR using the ratio method and differencing method (ratio_diff), 3) monthly GWR estimates and monthly adjusted estimates using ratio method (ratio_MAV). The differencing method and ratio method are shown in Eq. 4 and Eq. 5. Values were extracted at 77 thousand random points (Fig. A1) for year 2010. Values in ascending order were highlighted from white to red.

Fig. 4. (1) MSE-R^2 values (Eq. 1), (2) RMSE values (Eq. 2; unit: μg/m^3), and (3) relative RMSE values (Eq. 3) of LUR models for each calendar year using 5-fold CV. Annual LUR: annual estimates of the annual LUR models built in our previous study using GWR (Shen et al., 2022). Monthly LUR: annual average calculated from the monthly estimates of the monthly LUR models using GWR.

average observations from >5 % (up to 37 %) of the stations were only available for developing the monthly LURs and were unavailable for the annual LURs, as shown in Fig. A10. These extra observations could capture more spatial variations in the monthly air pollution, and thus the aggregated annual estimates from the monthly LUR could give more accurate spatial variations in the annual average concentrations than the annual LUR model estimates.

3.3. Monthly variations in LUR predictions

In general, spatial patterns were different across months for O_3, PM_{10} and $PM_{2.5}$ (Figs. 5–7), whereas for NO_2, some but less monthly variations can be found. Both the monthly averages and the contrasts between locations differed across months.

At a European scale (shown in Fig. 6), for NO_2, populated regions (mainly in Western and Central Europe and the Po Valley) had higher increases in estimated concentrations in winter and autumn than other regions. For O_3, Central and Southern Europe had higher estimates in summer than Northern Europe, whereas in winter western Europe had lower O_3 concentrations than other parts of Europe. For PM, the estimated concentrations in summer decreased more in Central, Eastern Europe and the Po Valley than in other regions. However, an increase in PM_{10} monthly concentrations was found in summer in Southwestern Europe (Spain, Italy, and Southern France).

Changes in Europe-wide monthly average concentrations are obvious during the period 2000–2019. For NO_2, the estimated monthly concentrations decreased for all months and regions (Fig. A14). For O_3, the monthly estimates increased especially in western, central and southern Europe in warm season (Fig. A16). For PM_{10}, the changes in monthly estimates were more dynamic than other pollutants but with an overall decreasing trend over years in all months (Fig. A18). The most substantial decrease in PM_{10} monthly concentrations was found in Spain and southern UK. For $PM_{2.5}$, from 2010 to 2019 an obvious decreasing trend was found as well (Fig. A20). A previous study in Switzerland also documents large seasonal variability in spatial patterns of $PM_{2.5}$ and PM_{10} concentrations (Eeftens et al., 2015).

At a city scale in Paris, monthly variations in air pollution patterns were also distinguishable (Fig. 7, A15, A17, A19, A21). Our estimated NO_2 maps showed local patterns from traffic emissions of vehicles, whereas O_3, PM_{10} and $PM_{2.5}$ maps showed more regional patterns.

3.4. Comparison of predictions at different spatial resolutions (25 m, 100 m, 1 km)

We compared our monthly LUR model predictions at three spatial resolutions (i.e., 25 m, 100 m, and 1 km) at a random point data set (77 thousand points across Europe). The overall Pearson's correlation of the predictions at the random points was very high between 25 m and 100 m predictions both across Europe (above 0.98 as shown in Fig. 8) and high in countries (above 0.876 as shown in Fig. A22) for all pollutants. The overall correlation was high between 25 m and 1 km predictions (above 0.91 as shown in Fig. 8) across Europe. The highest correlations were found for PM2.5 and PM10, pollutants with a relatively small local gradient. However, for some countries, the correlation values were moderate (0.4–0.8) between 25 m and 1 km predictions as shown in Fig. A22.

To visualize the changes in air pollution predictions at different scales, we plotted our air pollution prediction maps for a major city

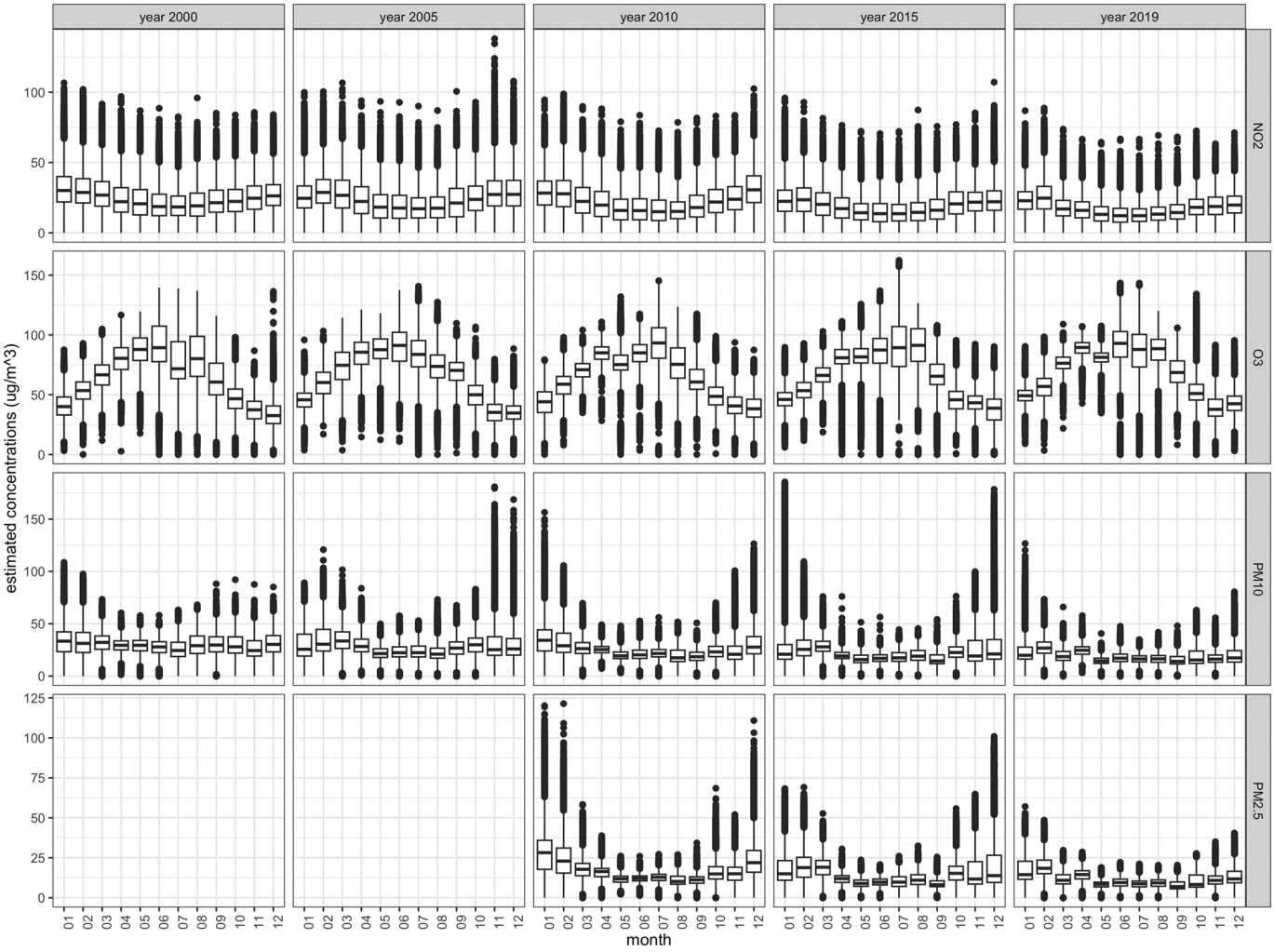

Fig. 5. Boxplots of monthly average ground-level concentrations (month 01–12) estimated by GWR for NO_2, O_3, PM_{10} and $PM_{2.5}$ in year 2000, 2005, 2010, 2015, and 2019 at 77 thousand random points (Fig. A1).

(Paris) at the different spatial resolutions in Figs. A23-A26. The near-roadway air pollution peaks were distinct at 25 m and 100 m. The 25 m and 100 m prediction maps in general showed similar locally-varying patterns. These patterns were reflected mainly by our selected land-use variables and road-related variables at a spatial resolution of either 100 m or 25 m, which represent the local variations in pollution emission sources (near-roadway, industrial- and residential emission sources). These local variations were not captured at a 1 km spatial resolution. The loss of local variation was also shown in Figs. A27-A30 where the air pollution predictions were extracted from the maps along a West-East transect in Paris.

The main application is in epidemiological studies. In epidemiological studies, residential addresses are commonly used to assess air pollution exposures, and previous studies have used these addresses to assign the exposures from 100 m annual average air pollution surfaces (Liu et al., 2021; Rodopoulou et al., 2022) or 1 km resolution (Brauer et al., 2022). The very high correlations between 25 m, 100 m, and 1 km resolution for $PM_{2.5}$ and PM_{10} indicate no clear benefit in using more detailed resolutions. For traffic-related pollutant NO_2, there is benefit using 25 m or 100 m instead of 1 km to represent near-roadway air pollution gradients. Based on the high correlation between the 25 m and 100 m resolution, results of epidemiological studies would likely have been similar. While 100 m prediction maps provide similar local patterns at a lower cost of computation resources, the 25 m prediction maps are an improvement for capturing locations of near-roadway air pollution. In studies of single urban areas, where the exposure contrast is more drive by near-roadway pollution, the benefit of 25 m resolution may be larger than in nation-wide or continental epidemiological studies.

In tracking studies where people's time-activity patterns are followed over time, a 25 m resolution might modestly improves assessment of commuting exposures over the larger resolutions. Monthly air pollution models are useful if the interest is in assessing average personal exposure, incorporating time activity patterns.

We observed a 10 %–20 % decrease in our NO_2 predictions within 40 m–80 m away from the roads in a specific small area in Paris. Previous studies have also shown a decline in air pollution concentrations with distance away from the road. Niepsch et al. (2022) shows that measured roadside NO2 concentrations peaked within 25 m away from the road and then decreased with 10 % and 20 % at distances of respectively 50 and 100 m. In their study, >30 % decrease in NO_2 concentrations was observed at 50 m away from nearby busy roads (with >30 thousand vehicles per day on average annually). Another study in the USA also found a 5 % decline in NO_2 concentrations with distance to the nearest highway using high spatial resolution of mobile data collected by vehicles on road (Apte et al., 2017).

It could be challenging to capture the variations at 25 m spatial resolution with a handful of observations compared to the total number of 25 m grid cells across Europe. However, the monitoring stations were a mix of roadside, urban background in larger and smaller cities and

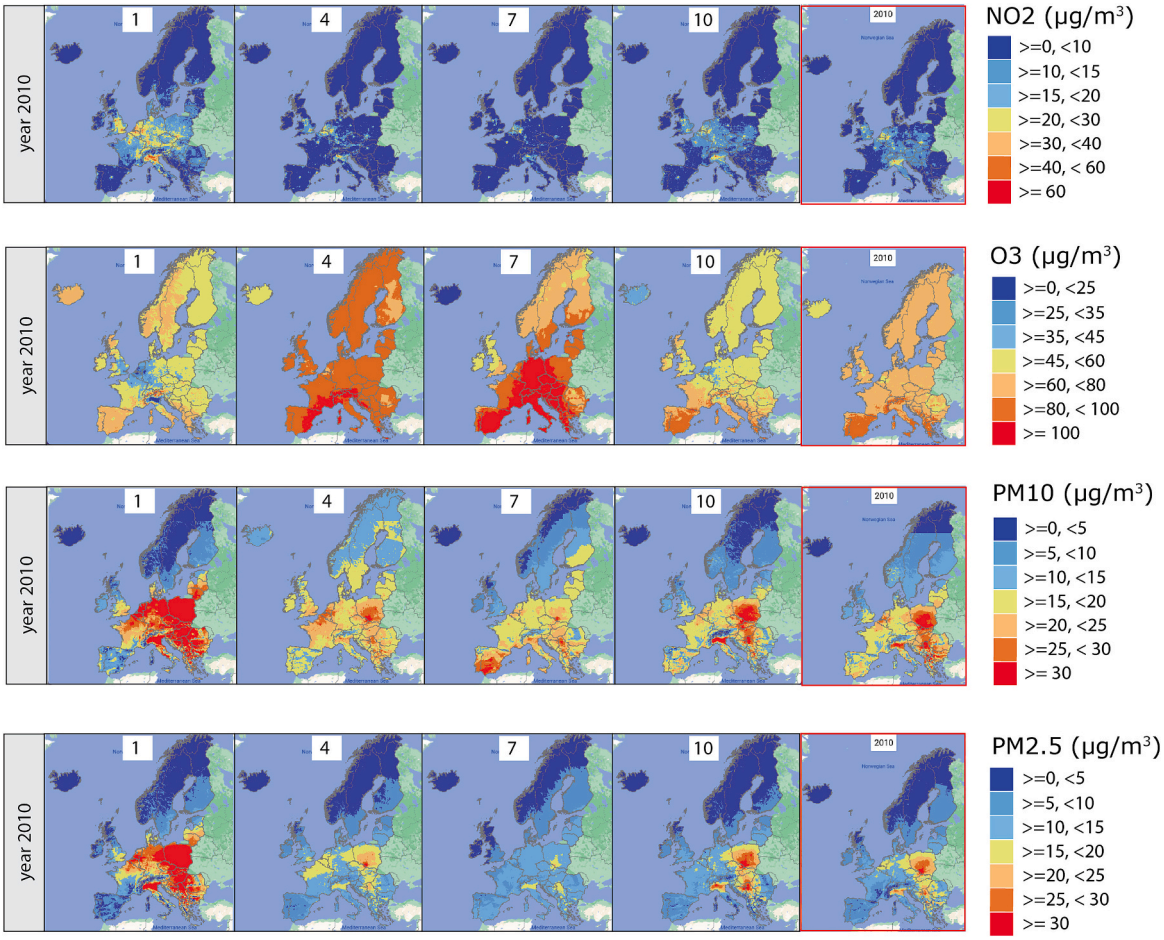

Fig. 6. Europe-wide monthly average maps of ground-level concentrations in μg/m^3 (for January: box '1', April: box '4', July: box '7', October: box '10') estimated by monthly GWR LUR and Europe-wide annual average maps (far right boxes bounded in red) estimated by annual GTWR LUR (Shen et al., 2022) for NO_2, O_3, PM_{10} and $PM_{2.5}$ in year 2010 at 25 m resolution (Base map source: Google Maps). The annual and monthly estimates of O_3 represent the annual and monthly average daily maximum 8-h mean. For other specific years (2000, 2005, 2015, 2019), readers are referred to Fig. A14, A16, A18, A20. For all years, visualization of monthly average estimated maps are available via https://youchenshenuu.users.earthengine.app/view/expanse-monthly-average-air-pollution-maps, and annual average estimated maps are available via https://youchenshenuu.users.earthengine.app/view/expanse-air-pollution-20-yr-maps.

regional background sites covering Europe. Moreover, our regression models selected the variables related to potential emission sources due to the variables' high contribution on explaining the spatial variations in observed air pollution, as shown and discussed in Section 3.1. The reliability of the models was further supported by the 5-fold CV using all hold-out observations. Evaluating LUR models with hold-out CV has been shown to reflect the predictive power even with small training datasets in 20 European study areas (Wang et al., 2013), because it can represent the locations where no measurements were taken. Thus, based on our 5-fold CV result, our regression models are able to capture variations in air pollution in different settings across Europe.

3.5. Limitation

Some improvements can be further achieved based on our monthly LUR models by including extra predictors and using spatio-temporal algorithms. Some satellite-retrieved data was excluded in our monthly LUR. The aerosol optical depth (AOD) retrieved by MODIS could help explaining more spatial variations in PM. Another satellite product from Tropospheric Monitoring Instrument (TROPOMI) has been available since 2018 with great improvement in spatial resolution from 13 × 24 km to 3.5 × 7 km compared to OMI. The atmospheric NO_2 column density from this TROPOMI could help capturing the variations in NO_2 and O_3 concentrations.

Moreover, in a handful of months, monthly LUR models exhibit more uncertainties, as indicated by the lower 5-fold CV R^2. Extra attention and care would be needed when the monthly exposure estimates are assigned in those time periods. For future studies, using spatiotemporal algorithms such as GTWR would help reducing the uncertainty in the estimates more than developing monthly specific LUR models. The GTWR could also solve the problem of limited $PM_{2.5}$ observations before 2006. Although our previous study shows that GWR and GTWR performed similarly annual, a previous study showed GTWR performed better than GWR at daily scale (He and Huang, 2018).

One could build daily LUR models to obtain monthly averages. However, building daily models with the method proposed in this study would entail extra uncertainties in estimates. To reduce the uncertainties, more temporally-resolved (daily) predictors are required. One of the main predictor variables in the daily air pollution models is satellite data, specifically Aerosol Optical Depth (AOD) for $PM_{2.5}$ and Ozone Monitoring Instrument (OMI) or Tropospheric Monitoring Instrument (TROPOMI) data for NO_2. The raw satellite data presents a substantial challenge due to the presence of significant data gaps contributed by factors such as cloud cover. To mitigate these data gaps before it can be used in the main modelling process, post-processing is required. It is a modelling stage whereby the missing data is filled through integrating information from chemical transport models and meteorological variables. The multi-stage modelling approach has been

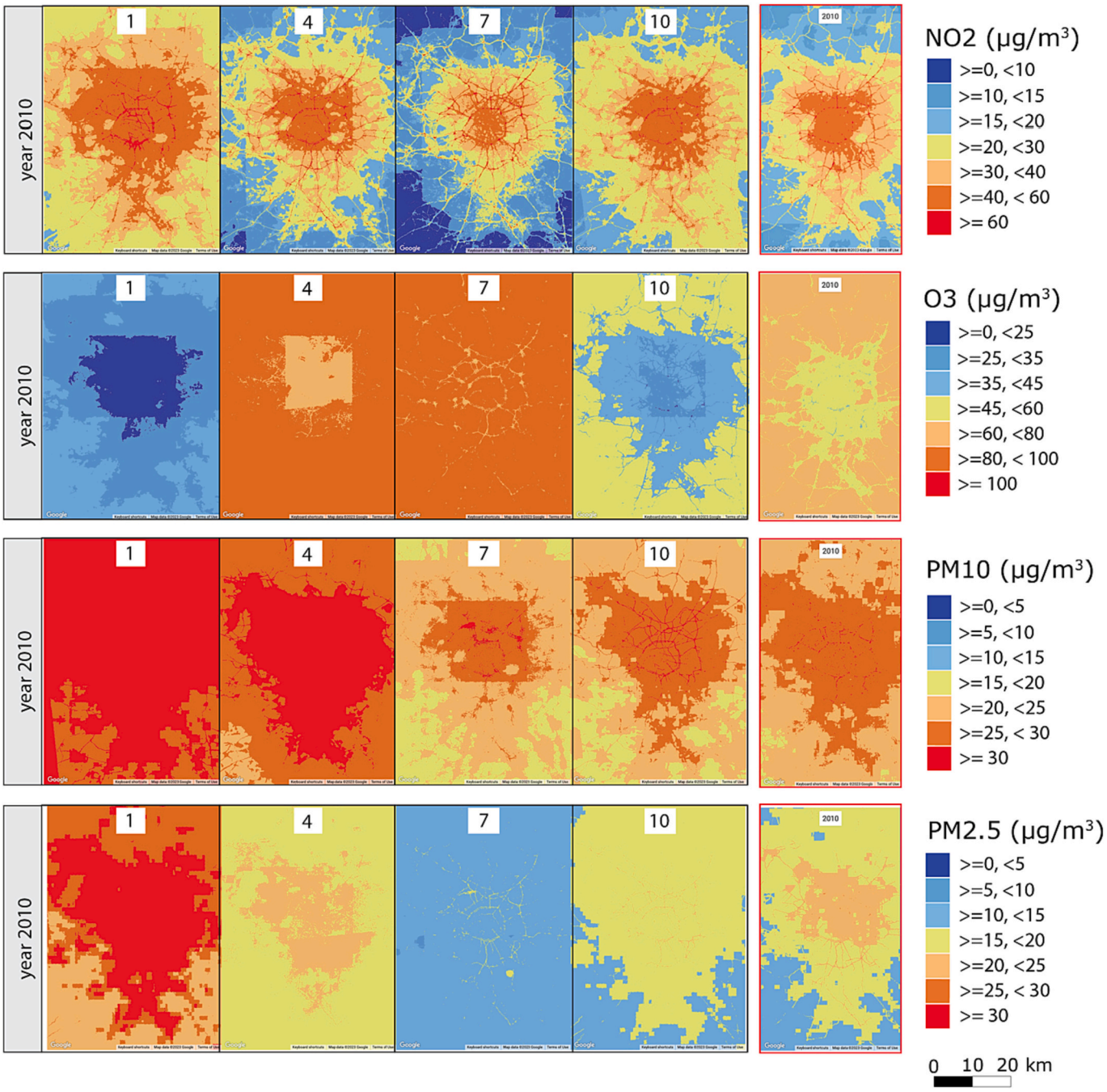

Fig. 7. Europe-wide monthly average maps of ground-level concentrations in μg/m^3 (for January: '1', April: '4', July: '7', October: '10') estimated by monthly GWR LUR and annual average (far right boxes bounded in red) estimated by annual GTWR LUR (Shen et al., 2022) for NO_2, O_3, PM_{10} and $PM_{2.5}$ in year 2010 in Paris at 25 m resolution. The annual and monthly estimates of O_3 represent the annual and monthly average daily maximum 8-h mean. For other specific years (2000, 2005, 2015, 2019), readers are referred to Fig. A15, A17, A19, A21. For all years, visualization of monthly average estimated maps are available via https://youchenshenuu.users.earthengine.app/view/expanse-monthly-average-air-pollution-maps, and annual average estimated maps are available via https://youchenshenuu.users.earthengine.app/view/expanse-air-pollution-20-yr-maps

applied in previous studies in Switzerland and Italy at 100 m spatial resolution as well as in North America and China at a 1 km resolution (de Hoogh et al., 2018b; De Hoogh et al., 2019; Di et al., 2019; Shao et al., 2020; Stafoggia et al., 2019; Wei et al., 2021; Wu et al., 2021).

Directly applying the methodology used in this study would therefore be inappropriate for building daily LUR models at a very fine spatial resolution. The prospect of building daily LUR models across Europe, with a focus on enhancing exposure assessment, is a topic worth exploring in future studies. However, it is essential to acknowledge that such an undertaking falls beyond the scope of this study. Given the need to balance between spatial and temporal resolution, we have chosen the approach of building monthly models exhibiting a notably high spatial resolution, as opposed to building daily models at a coarser spatial resolution.

4. Conclusion

Overall, the variations in monthly air pollution concentrations were substantial across most regions and months for most pollutants. Thus, we built Europe-wide monthly LUR models for each month during 20-

Fig. 8. Pearson's correlation of predictions at different scales (cor_25m100m: correlation between 25 m predictions and 100 m predictions; cor_25m1km: correlation between 25 m predictions and 1 km predictions) for NO2, O3, PM10 and PM2.5 in year 2000, 2005, 2010, 2015, and 2019 (by rows) in January (month 1), May (month 5), August (month 8), October (month 10) (by column).

year period. This is the first study that built monthly LUR models at fine spatial resolution (25 m) across Europe with generally good 5-fold CV accuracy. The model structures of the monthly LUR were different between months for O_3, PM_{10} and $PM_{2.5}$ with monthly-varying contribution from the selected variables. The resulting estimates showed large monthly-varying spatial patterns as well. In addition, aggregating the monthly LUR model estimates to annual averages slightly improved annual average estimates compared to the annual LUR model, because of the ability to capture within-year variations in the monthly LUR.

Moreover, the monthly LUR models outperformed the monthly-adjusted LUR models, but the correlation between monthly LUR and monthly-adjusted LUR were moderate to high. The findings indicate monthly LUR is preferable if possible, and monthly-adjusting method is acceptable albeit with higher uncertainty.

Our 25 m air pollution prediction maps show to capture the local traffic-related variations more accurately than the 100 m prediction maps based on visual inspection, although the overall correlation between the two was high (above 0.87).

To conclude, the resulting monthly LUR estimates can be used to identify the health effects of air pollution related to biological effects on intermediate-term effects and facilitate exploring critical exposure time-windows at a fine spatial resolution.

CRediT authorship contribution statement

Youchen Shen: Conceptualization, Formal analysis, Methodology, Writing – original draft. **Kees de Hoogh:** Conceptualization, Methodology, Supervision, Writing – review & editing. **Oliver Schmitz:** Data curation, Software, Writing – review & editing. **Nick Clinton:** Data curation, Software. **Karin Tuxen-Bettman:** Resources, Software. **Jørgen Brandt:** Data curation, Software, Writing – review & editing. **Jesper H. Christensen:** Data curation, Software, Writing – review & editing. **Lise M. Frohn:** Data curation, Software, Writing – review & editing. **Camilla Geels:** Data curation, Software, Writing – review & editing. **Derek Karssenberg:** Conceptualization, Methodology, Supervision, Writing – review & editing. **Roel Vermeulen:** Conceptualization, Funding acquisition, Supervision, Writing – review & editing. **Gerard Hoek:** Conceptualization, Methodology, Supervision, Writing – review & editing.

Declaration of competing interest

The authors declare that they have no known competing financial interests or personal relationships that could have appeared to influence the work reported in this paper.

Data availability

Data may be made available upon request.

Acknowledgement

This work was supported by EXPANSE and EXPOSOME-NL project. The EXPANSE project is funded by the European Union's Horizon 2020 research and innovation programme under grant agreement No 874627. The content of this article is not officially endorsed by the European

Union. The EXPOSOME-NL project is funded through the Gravitation program of the Dutch Ministry of Education, Culture, and Science and the Netherlands Organization for Scientific Research (NWO grant number 024.004.017). The computation was done with SURF Research Cloud infrastructure with grant no. SD-19729. The authors declare no competing financial interest.

Appendix A. Supplementary data

Supplementary data to this article can be found online at https://doi.org/10.1016/j.scitotenv.2024.170550.

References

Almeida, S.M., Manousakas, M., Diapouli, E., Kertesz, Z., Samek, L., Hristova, E., Šega, K., Alvarez, R.P., Belis, C.A., Eleftheriadis, K., Albania, Civici, N., Radic, R., Vukic, L., Hristova, E., Veleva, B., Šega, K., Bešlic, I., Davila, S., Godec, R., Manousakas, M., Diapouli, E., Vratolis, S., Eleftheriadis, K., Kertesz, Z., Belis, C.A., Bernatonis, M., Djukanovic, G., Jancic, D., Samek, L., Furman, L., Stegowski, Z., Almeida, S.M., Galinha, C., Balan, V., Nikolovska, L., Stefanovska, A., Radenkovic, M., Kneževic, J., Banu Oztas, N., Cantay, E., Turchenko, D.V., Abdullaev, S., Padilla Alvarez, R., Karydas, A.G., 2020. Ambient particulate matter source apportionment using receptor modelling in European and Central Asia urban areas. Environ. Pollut. 266, 115199 https://doi.org/10.1016/j.envpol.2020.115199.

Apte, J.S., Messier, K.P., Gani, S., Brauer, M., Kirchstetter, T.W., Lunden, M.M., Marshall, J.D., Portier, C.J., Vermeulen, R.C.H., Hamburg, S.P., 2017. High-resolution air pollution mapping with Google street view cars: exploiting big data. Environ. Sci. Technol. 51, 6999–7008. https://doi.org/10.1021/acs.est.7b00891.

Araki, S., Shima, M., Yamamoto, K., 2020. Estimating historical PM2.5 exposures for three decades (1987–2016) in Japan using measurements of associated air pollutants and land use regression. Environ. Pollut. 263, 114476 https://doi.org/10.1016/j.envpol.2020.114476.

Barmpadimos, I., Hueglin, C., Keller, J., Henne, S., Prévôt, A.S.H., 2011. Influence of meteorology on PM10 trends and variability in Switzerland from 1991 to 2008. Atmos. Chem. Phys. 11, 1813–1835. https://doi.org/10.5194/acp-11-1813-2011.

Barmpadimos, I., Keller, J., Oderbolz, D., Hueglin, C., Prévôt, A.S.H., 2012. One decade of parallel fine (PM 2.5) and coarse (PM 10-PM 2.5) particulate matter measurements in Europe: trends and variability. Atmos. Chem. Phys. 12, 3189–3203. https://doi.org/10.5194/acp-12-3189-2012.

Basso, K., De Avila Zingano, P.R., Dal Sasso Freitas, C.M., 1999. Interpolation of scattered data: Investigating alternatives for the modified Shepard method. In: Proceedings - 12th Brazilian Symposium on Computer Graphics and Lmage Processing, SIBGRAPI 1999. Institute of Electrical and Electronics Engineers Inc., pp. 39–47. https://doi.org/10.1109/SIBGRA.1999.805606

Bauwelinck, M., Chen, J., de Hoogh, K., Katsouyanni, K., Rodopoulou, S., Samoli, E., Andersen, Z.J., Atkinson, R., Casas, L., Deboosere, P., Demoury, C., Janssen, N., Klompmaker, J.O., Lefebvre, W., Mehta, A.J., Nawrot, T.S., Oftedal, B., Renzi, M., Stafoggia, M., Strak, M., Vandenheede, H., Vanpoucke, C., Van Nieuwenhuyse, A., Vienneau, D., Brunekreef, B., Hoek, G., 2022. Variability in the association between long-term exposure to ambient air pollution and mortality by exposure assessment method and covariate adjust- ment: a census-based country-wide cohort study. Sci. Total Environ. 804, 150091 https://doi.org/10.1016/j.scitotenv.2021.150091.

Bechle, M.J., Millet, D.B., Marshall, J.D., 2015. National Spatiotemporal exposure surface for NO2: monthly scaling of a satellite-derived land-use regression, 2000-2010. Environ. Sci. Technol. 49, 12297–12305. https://doi.org/10.1021/acs.est.5b02882.

Beckerman, B.S., Jerrett, M., Serre, M., Martin, R.V., Lee, S.J., Van Donkelaar, A., Ross, Z., Su, J., Burnett, R.T., 2013. A hybrid approach to estimating national scale spatiotemporal variability of PM2.5 in the contiguous United States. Environ. Sci. Technol. 47, 7233–7241. https://doi.org/10.1021/es400039u.

Beelen, R., Stafoggia, M., Raaschou-Nielsen, O., Andersen, Z.J., Xun, W.W., Katsouyanni, K., Dimakopoulou, K., Brunekreef, B., Weinmayr, G., Hoffmann, B., Wolf, K., Samoli, E., Houthuijs, D., Nieuwenhuijsen, M., Oudin, A., Forsberg, B., Olsson, D., Salomaa, V., Lanki, T., Yli-Tuomi, T., Oftedal, B., Aamodt, G., Nafstad, P., De Faire, U., Pedersen, N.L., Östenson, C.G., Fratiglioni, L., Penell, J., Korek, M., Pyko, A., Eriksen, K.T., Tjønneland, A., Becker, T., Eeftens, M., Bots, M., Meliefste, K., Wang, M., Bueno-De-Mesquita, B., Sugiri, D., Krämer, U., Heinrich, J., De Hoogh, K., Key, T., Peters, A., Cyrys, J., Concin, H., Nagel, G., Ineichen, A., Schaffner, E., Probst-Hensch, N., Dratva, J., Ducret-Stich, R., Vilier, A., Clavel-Chapelon, F., Stempfelet, M., Grioni, S., Krogh, V., Tsai, M.Y., Marcon, A., Ricceri, F., Sacerdote, C., Galassi, C., Migliore, E., Ranzi, A., Cesaroni, G., Badaloni, C., Forastiere, F., Tamayo, I., Amiano, P., Dorronsoro, M., Katsoulis, M., Trichopoulou, A., Vineis, P., Hoek, G., 2014. Long-term exposure to air pollution and cardiovascular mortality: an analysis of 22 European cohorts. Epidemiology 25, 368–378. https://doi.org/10.1097/EDE.000000 0000000076.

Bowe, B., Xie, Y., Li, T., Yan, Y., Xian, H., Al-Aly, Z., 2018. The 2016 global and national burden of diabetes mellitus attributable to PM 2·5 air pollution. Lancet Planet. Heal. 2, e301–e312. https://doi.org/10.1016/S2542-5196(18)30140-2.

Brandt, J., Silver, J.D., Frohn, L.M., Geels, C., Gross, A., Hansen, A.B., Hansen, K.M., Hedegaard, G.B., Skjøth, C.A., Villadsen, H., Zare, A., Christensen, J.H., 2012. An integrated model study for Europe and North America using the Danish Eulerian hemispheric model with focus on intercontinental transport of air pollution. Atmos. Environ. 53, 156–176. https://doi.org/10.1016/j.atmosenv.2012.01.011.

Brauer, M., Brook, J.R., Christidis, T., Chu, Y., Crouse, D.L., Erickson, A., Hystad, P., Li, C., Martin, R.V., Jun Meng, A., Pappin, J., Pinault, L.L., Tjepkema, M., van Donkelaar, A., Weagle, C., Weichenthal, S., Burnett, R.T., 2022. Mortality–Air Pollution Associations in Low-Exposure Environments (MAPLE): Phase 2. Health Effects Institute, HEI.

Brunsdon, C., Fotheringham, A.S., Charlton, M.E., 1996. Geographically weighted regression: a method for exploring spatial nonstationarity. Geogr. Anal. 28, 281–298. https://doi.org/10.1111/j.1538-4632.1996.tb00936.x.

Cakmak, S., Hebbern, C., Vanos, J., Crouse, D.L., Burnett, R., 2016. Ozone exposure and cardiovascular-related mortality in the Canadian census health and environment cohort (CANCHEC) by spatial synoptic classification zone. Environ. Pollut. 214, 589–599. https://doi.org/10.1016/j.envpol.2016.04.067.

Cakmak, S., Hebbern, C., Pinault, L., Lavigne, E., Vanos, J., Crouse, D.L., Tjepkema, M., 2018. Associations between long-term PM2.5 and ozone exposure and mortality in the Canadian census health and environment cohort (CANCHEC), by spatial synoptic classification zone. Environ. Int. 111, 200–211. https://doi.org/10.1016/j.envint.2017.11.030.

Chen, J., de Hoogh, K., Gulliver, J., Hoffmann, B., Hertel, O., Ketzel, M., Bauwelinck, M., van Donkelaar, A., Hvidtfeldt, U.A., Katsouyanni, K., Janssen, N.A.H., Martin, R.V., Samoli, E., Schwartz, P.E., Stafoggia, M., Bellander, T., Strak, M., Wolf, K., Vienneau, D., Vermeulen, R., Brunekreef, B., Hoek, G., 2019. A comparison of linear regression, regularization, and machine learning algorithms to develop Europe-wide spatial models of fine particles and nitrogen dioxide. Environ. Int. 130, 104934 https://doi.org/10.1016/j.envint.2019.104934.

Chen, J., Rodopoulou, S., de Hoogh, K., Strak, M., Andersen, Z.J., Atkinson, R., Bauwelinck, M., Bellander, T., Brandt, J., Cesaroni, G., Concin, H., Fecht, D., Forastiere, F., Gulliver, J., Hertel, O., Hoffmann, B., Hvidtfeldt, U.A., Janssen, N.A.H., Jöckel, K.H., Jørgensen, J., Katsouyanni, K., Ketzel, M., Klompmaker, J.O., Lager, A., Leander, K., Liu, S., Ljungman, P., Macdonald, C.J., Magnusson, P.K.E., Mehta, A., Nagel, G., Oftedal, B., Pershagen, G., Peters, A., Raaschou-Nielsen, O., Renzi, M., Rizzuto, D., Samoli, E., van der Schouw, Y.T., Schramm, S., Schwarze, P., Sigsgaard, T., Sørensen, M., Stafoggia, M., Tjønneland, A., Vienneau, D., Weinmayr, G., Wolf, K., Brunekreef, B., Hoek, G., 2021. Long-term exposure to fine particle elemental components and natural and cause-specific mortality—a pooled analysis of eight european cohorts within the ELAPSE project. Environ. Health Perspect. 129 https://doi.org/10.1289/EHP8368.

Copernicus, 2021. Imperviousness [WWW Document]. Copernicus Progr. URL. https://land.copernicus.eu/pan-european/high-resolution-layers/imperviousness (accessed 3.9.21).

de Hoogh, K., Chen, J., Gulliver, J., Hoffmann, B., Hertel, O., Ketzel, M., Bauwelinck, M., van Donkelaar, A., Hvidtfeldt, U.A., Katsouyanni, K., Klompmaker, J., Martin, R.V., Samoli, E., Schwartz, P.E., Stafoggia, M., Bellander, T., Strak, M., Wolf, K., Vienneau, D., Brunekreef, B., Hoek, G., 2018a. Spatial PM2.5, NO2, O3 and BC models for Western Europe – evaluation of spatiotemporal stability. Environ. Int. 120, 81–92. https://doi.org/10.1016/j.envint.2018.07.036.

de Hoogh, K., Héritier, H., Stafoggia, M., Künzli, N., Kloog, I., 2018b. Modelling daily PM2.5 concentrations at high spatio-temporal resolution across Switzerland. Environ. Pollut. 233, 1147–1154. https://doi.org/10.1016/j.envpol.2017.10.025.

De Hoogh, K., Saucy, A., Shtein, A., Schwartz, J., West, E.A., Strassmann, A., Puhan, M., Roösli, M., Stafoggia, M., Kloog, I., 2019. Predicting fine-scale daily NO2 for 2005-2016 incorporating OMI satellite data across Switzerland. Environ. Sci. Technol. 53, 10279–10287. https://doi.org/10.1021/acs.est.9b03107.

Di, Q., Wang, Yan, Zanobetti, A., Wang, Yun, Koutrakis, P., Choirat, C., Dominici, F., Schwartz, J.D., 2017. Air pollution and mortality in the Medicare population. N. Engl. J. Med. 376, 2513–2522. https://doi.org/10.1056/nejmoa1702747.

Di, Q., Amini, H., Shi, L., Kloog, I., Silvern, R., Kelly, J., Sabath, M.B., Choirat, C., Koutrakis, P., Lyapustin, A., Wang, Y., Mickley, L.J., Schwartz, J., 2019. An ensemble-based model of PM2.5 concentration across the contiguous United States with high spatiotemporal resolution. Environ. Int. 130, 104909 https://doi.org/10.1016/j.envint.2019.104909.

Duncan, B.N., Bey, I., 2004. A modeling study of the export pathways of pollution from Europe: seasonal and interannual variations (1987–1997). J. Geophys. Res. D Atmos. 109 https://doi.org/10.1029/2003JD004079.

Eckel, S.P., Cockburn, M., Shu, Y.H., Deng, H., Lurmann, F.W., Liu, L., Gilliland, F.D., 2016. Air pollution affects lung cancer survival. Thorax 71, 891–898. https://doi.org/10.1136/thoraxjnl-2015-207927.

Eeftens, M., Beelen, R., De Hoogh, K., Bellander, T., Cesaroni, G., Cirach, M., Declercq, C., Dedele, A., Dons, E., De Nazelle, A., Dimakopoulou, K., Eriksen, K., Falq, G., Fischer, P., Galassi, C., Gražulevičiene, R., Heinrich, J., Hoffmann, B., Jerrett, M., Keidel, D., Korek, M., Lanki, T., Lindley, S., Madsen, C., Mölter, A., Nádor, G., Nieuwenhuijsen, M., Nonnemacher, M., Pedeli, X., Raaschou-Nielsen, O., Patelarou, E., Quass, U., Ranzi, A., Schindler, C., Stempfelet, M., Stephanou, E., Sugiri, D., Tsai, M.Y., Yli-Tuomi, T., Varró, M.J., Vienneau, D., Von Klot, S., Wolf, K., Brunekreef, B., Hoek, G., 2012. Development of land use regression models for PM2.5, PM 2.5 absorbance, PM10 and PMcoarse in 20 European study areas; results of the ESCAPE project. Environ. Sci. Technol. 46, 11195–11205. https://doi.org/10.1021/es301948k.

Eeftens, M., Phuleria, H.C., Meier, R., Aguilera, I., Corradi, E., Davey, M., Ducret-Stich, R., Fierz, M., Gehrig, R., Ineichen, A., Keidel, D., Probst-Hensch, N., Ragettli, M.S., Schindler, C., Künzli, N., Tsai, M.Y., 2015. Spatial and temporal variability of ultrafine particles, NO2, PM2.5, PM2.5 absorbance, PM10 and PMcoarse in Swiss study areas. Atmos. Environ. 111, 60–70. https://doi.org/10.1016/j.atmosenv.2015.03.031.

European Environment Agency, 2021. Classification of monitoring stations and criteria to include them in EEA's assessments products Related content Related briefings [WWW Document]. https://www.eea.europa.eu/themes/air/air-quality-concentrations/classification-of-monitoring-stations-and.

EUROSTAT, 2021. GISCO statistical unit dataset: NUTS [WWW Document]. https://ec.europa.eu/eurostat/web/gisco/geodata/reference-data/administrative-units-statistical-units/nuts (accessed 5.11.23).

Fouladi, F., Bailey, M.J., Patterson, W.B., Sioda, M., Blakley, I.C., Fodor, A.A., Jones, R. B., Chen, Z., Kim, J.S., Lurmann, F., Martino, C., Knight, R., Gilliland, F.D., Alderete, T.L., 2020. Air pollution exposure is associated with the gut microbiome as revealed by shotgun metagenomic sequencing. Environ. Int. 138 https://doi.org/10.1016/j.envint.2020.105604.

Frohn, L.M., Geels, C., Andersen, C., Andersson, C., Bennet, C., Christensen, J.H., Im, U., Karvosenoja, N., Kindler, P.A., Kukkonen, J., Lopez-Aparicio, S., Nielsen, O.K., Palamarchuk, Y., Paunu, V.V., Plejdrup, M.S., Segersson, D., Sofiev, M., Brandt, J., 2022. Evaluation of multidecadal high-resolution atmospheric chemistry-transport modelling for exposure assessments in the continental Nordic countries. Atmos. Environ. 290, 119334 https://doi.org/10.1016/J.ATMOSENV.2022.119334.

Giordano, L., Brunner, D., Flemming, J., Hogrefe, C., Im, U., Bianconi, R., Badia, A., Balzarini, A., Baró, R., Chemel, C., Curci, G., Forkel, R., Jiménez-Guerrero, P., Hirtl, M., Hodzic, A., Honzak, L., Jorba, O., Knote, C., Kuenen, J.J.P., Makar, P.A., Manders-Groot, A., Neal, L., Pérez, J.L., Pirovano, G., Pouliot, G., San José, R., Savage, N., Schröder, W., Sokhi, R.S., Syrakov, D., Torian, A., Tuccella, P., Werhahn, J., Wolke, R., Yahya, K., Žabkar, R., Zhang, Y., Galmarini, S., 2015. Assessment of the MACC reanalysis and its influence as chemical boundary conditions for regional air quality modeling in AQMEII-2. Atmos. Environ. 115, 371–388. https://doi.org/10.1016/j.atmosenv.2015.02.034.

Gollini, I., Lu, B., Charlton, M., Brunsdon, C., Harris, P., 2015. {GWmodel}: an {R} package for exploring spatial heterogeneity using geographically weighted models. J. Stat. Softw. 63, 1–50.

Gondalia, R., Baldassari, A., Holliday, K.M., Justice, A.E., Stewart, J.D., Liao, D., Yanosky, J.D., Engel, S.M., Sheps, D., Jordahl, K.M., Bhatti, P., Horvath, S., Assimes, T.L., Demerath, E.W., Guan, W., Fornage, M., Bressler, J., North, K.E., Conneely, K.N., Li, Y., Hou, L., Baccarelli, A.A., Whitsel, E.A., 2021. Epigenetically mediated electrocardiographic manifestations of sub-chronic exposures to ambient particulate matter air pollution in the Women's Health Initiative and atherosclerosis risk in communities study. Environ. Res. 198, 111211 https://doi.org/10.1016/J.ENVRES.2021.111211.

Gorelick, N., Hancher, M., Dixon, M., Ilyushchenko, S., Thau, D., Moore, R., 2017. Google earth engine: planetary-scale geospatial analysis for everyone. Remote Sens. Environ. 202, 18–27. https://doi.org/10.1016/j.rse.2017.06.031.

Guevara, M., Jorba, O., Tena, C., Denier Van Der Gon, H., Kuenen, J., Elguindi, N., Darras, S., Granier, C., Pérez García-Pando, C., 2021. Copernicus atmosphere monitoring service TEMPOral profiles (CAMS-TEMPO): global and European emission temporal profile maps for atmospheric chemistry modelling. Earth Syst. Sci. Data 13, 367–404. https://doi.org/10.5194/essd-13-367-2021.

Gulliver, J., De Hoogh, K., Hansell, A., Vienneau, D., 2013. Development and back-extrapolation of NO2 land use regression models for historic exposure assessment in Great Britain. Environ. Sci. Technol. 47, 7804–7811. https://doi.org/10.1021/es4008849.

Hammer, M.S., Van Donkelaar, A., Li, C., Lyapustin, A., Sayer, A.M., Hsu, N.C., Levy, R. C., Garay, M.J., Kalashnikova, O.V., Kahn, R.A., Brauer, M., Apte, J.S., Henze, D.K., Zhang, L., Zhang, Q., Ford, B., Pierce, J.R., Martin, R.V., 2020. Global estimates and long-term trends of fine particulate matter concentrations (1998–2018). Environ. Sci. Technol. 54, 7879–7890. https://doi.org/10.1021/acs.est.0c01764.

Hannam, K., McNamee, R., De Vocht, F., Baker, P., Sibley, C., Agius, R., 2013. A comparison of population air pollution exposure estimation techniques with personal exposure estimates in a pregnant cohort. Environ Sci Process Impacts 15, 1562–1572. https://doi.org/10.1039/c3em00112a.

He, Q., Huang, B., 2018. Satellite-based high-resolution PM2.5 estimation over the Beijing-Tianjin-Hebei region of China using an improved geographically and temporally weighted regression model. Environ. Pollut. 236, 1027–1037. https://doi.org/10.1016/j.envpol.2018.01.053.

HEI, 2022. Systematic review and meta-analysis of selected health effects of long-term exposure to traffic-related air pollution HEI panel on the health effects of long-term exposure to traffic-related air pollution health effects institute.e.

Hoek, G., 2017. Methods for assessing long-term exposures to outdoor air pollutants. Curr. Environ. Heal. Reports 4, 450–462. https://doi.org/10.1007/s40572-017-0169-5.

Iñiguez, C., Ballester, F., Estarlich, M., Esplugues, A., Murcia, M., Llop, S., Plana, A., Amorós, R., Rebagliato, M., 2012. Prenatal exposure to traffic-related air pollution and fetal growth in a cohort of pregnant women. Occup. Environ. Med. 69, 736–744. https://doi.org/10.1136/oemed-2011-100550.

Iñiguez, C., Esplugues, A., Sunyer, J., Basterrechea, M., Fernández-Somoano, A., Costa, O., Estarlich, M., Aguilera, I., Lertxundi, A., Tardón, A., Guxens, M., Murcia, M., Lopez-Espinosa, M.J., Ballester, F., 2016. Prenatal exposure to NO2 and ultrasound measures of fetal growth in the Spanish INMA cohort. Environ. Health Perspect. 124, 235–242. https://doi.org/10.1289/ehp.1409423.

Ito, K., De Leon, S., Thurston, G.D., Nadas, A., Lippmann, M., 2005. Monitor-to-monitor temporal correlation of air pollution in the contiguous US. J. Expo. Anal. Environ. Epidemiol. 15, 172–184. https://doi.org/10.1038/sj.jea.7500386.

Jerrett, M., Arain, A., Kanaroglou, P., Beckerman, B., Potoglou, D., Sahsuvaroglu, T., Morrison, J., Giovis, C., 2005. A review and evaluation of intraurban air pollution exposure models. J. Expo. Anal. Environ. Epidemiol. https://doi.org/10.1038/sj.jea.7500388.

Jiang, W., Liu, Z., Ni, B., Xie, W., Zhou, H., Li, X., 2021. Independent and interactive effects of air pollutants and ambient heat exposure on congenital heart defects. Reprod. Toxicol. 104, 106–113. https://doi.org/10.1016/J.REPROTOX.2021.07.007.

Juda-Rezler, K., Reizer, M., Maciejewska, K., Błaszczak, B., Klejnowski, K., 2020. Characterization of atmospheric PM2.5 sources at a central European urban background site. Sci. Total Environ. 713, 136729 https://doi.org/10.1016/j.scitotenv.2020.136729.

Kim, J.S., Chen, Z., Alderete, T.L., Toledo-Corral, C., Lurmann, F., Berhane, K., Gilliland, F.D., 2019a. Associations of AIR pollution, obesity and cardiometabolic health in young adults: the Meta-AIR study. Environ. Int. 133, 105180 https://doi.org/10.1016/j.envint.2019.105180.

Kim, H., Kim, Hyomi, Lee, J.T., 2019b. Spatial variation in lag structure in the short-term effects of air pollution on mortality in seven major south Korean cities, 2006–2013. Environ. Int. 125, 595–605. https://doi.org/10.1016/j.envint.2018.09.004.

Knibbs, L.D., Hewson, M.G., Bechle, M.J., Marshall, J.D., Barnett, A.G., 2014. A national satellite-based land-use regression model for air pollution exposure assessment in Australia. Environ. Res. 135, 204–211. https://doi.org/10.1016/j.envres.2014.09.011.

Liu, S., Jørgensen, J.T., Ljungman, P., Pershagen, G., Bellander, T., Leander, K., Magnusson, P.K.E., Rizzuto, D., Hvidtfeldt, U.A., Raaschou-Nielsen, O., Wolf, K., Hoffmann, B., Brunekreef, B., Strak, M., Chen, J., Mehta, A., Atkinson, R.W., Bauwelinck, M., Varraso, R., Boutron-Ruault, M.C., Brandt, J., Cesaroni, G., Forastiere, F., Fecht, D., Gulliver, J., Hertel, O., de Hoogh, K., Janssen, N.A.H., Katsouyanni, K., Ketzel, M., Klompmaker, J.O., Nagel, G., Oftedal, B., Peters, A., Tjønneland, A., Rodopoulou, S.P., Samoli, E., Bekkevold, T., Sigsgaard, T., Stafoggia, M., Vienneau, D., Weinmayr, G., Hoek, G., Andersen, Z.J., 2021. Long-term exposure to low-level air pollution and incidence of chronic obstructive pulmonary disease: the ELAPSE project. Environ. Int. 146, 106267 https://doi.org/10.1016/j.envint.2020.106267.

Lu, B., Harris, P., Charlton, M., Brunsdon, C., 2014. The {GWmodel} {R} package: further topics for exploring spatial heterogeneity using geographically weighted models. Geo-spatial Inf. Sci. 17, 85–101.

Lu, M., Soenario, I., Helbich, M., Schmitz, O., Hoek, G., van der Molen, M., Karssenberg, D., 2020. Land use regression models revealing spatiotemporal co-variation in NO2, NO, and O3 in the Netherlands. Atmos. Environ. 223, 117238 https://doi.org/10.1016/j.atmosenv.2019.117238.

Lu, J., Zhang, Y., Chen, M., Wang, L., Zhao, S., Pu, X., Chen, X., 2021. Estimation of monthly 1 km resolution PM2.5 concentrations using a random forest model over "2 + 26" cities, China. Urban Clim. 35, 100734 https://doi.org/10.1016/j.uclim.2020.100734.

Marécal, V., Peuch, V.H., Andersson, C., Andersson, S., Arteta, J., Beekmann, M., Benedictow, A., Bergström, R., Bessagnet, B., Cansado, A., Chéroux, F., Colette, A., Coman, A., Curier, R.L., Van Der Gon, H.A.C.D., Drouin, A., Elbern, H., Emili, E., Engelen, R.J., Eskes, H.J., Foret, G., Friese, E., Gauss, M., Giannaros, C., Guth, J., Joly, M., Jaumouillé, E., Josse, B., Kadygrov, N., Kaiser, J.W., Krajsek, K., Kuenen, J., Kumar, U., Liora, N., Lopez, E., Malherbe, L., Martinez, I., Melas, D., Meleux, F., Menut, L., Moinat, P., Morales, T., Parmentier, J., Piacentini, A., Plu, M., Poupkou, A., Queguiner, S., Robertson, L., Rouïl, L., Schaap, M., Segers, A., Sofiev, M., Tarasson, L., Thomas, M., Timmermans, R., Valdebenito, Van Velthoven, P., Van Versendaal, R., Vira, J., Ung, A., 2015. A regional air quality forecasting system over Europe: the MACC-II daily ensemble production. Geosci. Model Dev. 8, 2777–2813. https://doi.org/10.5194/gmd-8-2777-2015.

Morawska, L., Zhu, T., Liu, N., Amouei Torkmahalleh, M., de Fatima Andrade, M., Barratt, B., Broomandi, P., Buonanno, G., Ceron, Carlos Belalcazar, Chen, J., Cheng, Y., Evans, G., Gavidia, M., Guo, H., Hanigan, I., Hu, M., Jeong, C.H., Kelly, F., Gallardo, L., Kumar, P., Lyu, X., Mullins, B.J., Nordstrøm, C., Pereira, G., Querol, X., Yezid Rojas Roa, N., Russell, A., Thompson, H., Wang, H., Wang, L., Wang, T., Wierzbicka, A., Xue, T., Ye, C., 2021. The state of science on severe air pollution episodes: quantitative and qualitative analysis. Environ. Int. 156 https://doi.org/10.1016/j.envint.2021.106732.

Mortimer, K., Neugebauer, R., Lurmann, F., Alcorn, S., Balmes, J., Tager, I., 2008. Air pollution and pulmonary function in asthmatic children effects of prenatal and lifetime exposures. Epidemiology 19, 550–557. https://doi.org/10.1097/EDE.0B013E31816A9DCB.

Niepsch, D., Clarke, L.J., Tzoulas, K., Cavan, G., 2022. Spatiotemporal variability of nitrogen dioxide (NO2) pollution in Manchester (UK) city centre (2017–2018) using a fine spatial scale single-NOx diffusion tube network. Environ. Geochem. Health 44, 3907–3927. https://doi.org/10.1007/S10653-021-01149-W/FIGURES/6.

Ordónez, C., Mathis, H., Furger, M., Henne, S., Hüglin, C., Staehelin, J., Prévôt, A.S.H., 2005. Changes of daily surface ozone maxima in Switzerland in all seasons from 1992 to 2002 and discussion of summer 2003. Atmos. Chem. Phys. 5, 1187–1203. https://doi.org/10.5194/acp-5-1187-2005.

Pappin, A.J., Christidis, T., Pinault, L.L., Crouse, D.L., Brook, J.R., Erickson, A., Hystad, P., Li, C., Martin, R.V., Meng, J., Weichenthal, S., van Donkelaar, A., Tjepkema, M., Brauer, M., Burnett, R.T., 2019. Examining the shape of the association between low levels of fine particulate matter and mortality across three cycles of the Canadian census health and environment cohort. Environ. Health Perspect. 127 https://doi.org/10.1289/EHP5204.

Patterson, W.B., Glasson, J., Naik, N., Jones, R.B., Berger, P.K., Plows, J.F., Minor, H.A., Lurmann, F., Goran, M.I., Alderete, T.L., 2021. Prenatal exposure to ambient air pollutants and early infant growth and adiposity in the Southern California mother's milk study. Environ. Heal. A Glob. Access Sci. Source 20, 1–12. https://doi.org/10.1186/s12940-021-00753-8.

Pedersen, M., Giorgis-Allemand, L., Bernard, C., Aguilera, I., Andersen, A.M.N., Ballester, F., Beelen, R.M.J., Chatzi, L., Cirach, M., Danileviciute, A., Dedele, A., van

Eijsden, M., Estarlich, M., Fernández-Somoano, A., Fernández, M.F., Forastiere, F., Gehring, U., Grazuleviciene, R., Gruzieva, O., Heude, B., Hoek, G., de Hoogh, K., van den Hooven, E.H., Håberg, S.E., Jaddoe, V.W.V., Klümper, C., Korek, M., Krämer, U., Lerchundi, A., Lepeule, J., Nafstad, P., Nystad, W., Patelarou, E., Porta, D., Postma, D., Raaschou-Nielsen, O., Rudnai, P., Sunyer, J., Stephanou, E., Sørensen, M., Thiering, E., Tuffnell, D., Varró, M.J., Vrijkotte, T.G.M., Wijga, A., Wilhelm, M., Wright, J., Nieuwenhuijsen, M.J., Pershagen, G., Brunekreef, B., Kogevinas, M., Slama, R., 2013. Ambient air pollution and low birthweight: a European cohort study (ESCAPE). Lancet Respir. Med. 1, 695–704. https://doi.org/10.1016/S2213-2600(13)70192-9.

Pedersen, M., Gehring, U., Beelen, R., Wang, M., Giorgis-Allemand, L., Andersen, A.M.N., Basagaña, X., Bernard, C., Cirach, M., Forastiere, F., De Hoogh, K., Gražulevičvienė, R., Gruzieva, O., Hoek, G., Jedynska, A., Klümper, C., Kooter, I.M., Krämer, U., Kukkonen, J., Porta, D., Postma, D.S., Raaschou-Nielsen, O., Van Rossem, L., Sunyer, J., Sørensen, M., Tsai, M.Y., Vrijkotte, T.G.M., Wilhelm, M., Nieuwenhuijsen, M.J., Pershagen, G., Brunekreef, B., Kogevinas, M., Slama, R., 2016. Elemental constituents of particulate matter and newborn's size in eight European cohorts. Environ. Health Perspect. 124, 141–150. https://doi.org/10.1289/ehp.1409546.

Pinault, L.L., Weichenthal, S., Crouse, D.L., Brauer, M., Erickson, A., van Donkelaar, A., Martin, R.V., Hystad, P., Chen, H., Finès, P., Brook, J.R., Tjepkema, M., Burnett, R.T., 2017. Associations between fine particulate matter and mortality in the 2001 Canadian Census Health and Environment Cohort. Environ. Res. 159, 406–415. https://doi.org/10.1016/j.envres.2017.08.037.

Power, M.C., Kioumourtzoglou, M.A., Hart, J.E., Okereke, O.I., Laden, F., Weisskopf, M. G., 2015. The relation between past exposure to fine particulate air pollution and prevalent anxiety: observational cohort study. BMJ 350. https://doi.org/10.1136/bmj.h1111.

Proietti, E., Delgado-Eckert, E., Vienneau, D., Stern, G., Tsai, M.Y., Latzin, P., Frey, U., Röösli, M., 2016. Air pollution modelling for birth cohorts: a time-space regression model. Environ. Heal. A Glob. Access Sci. Source 15. https://doi.org/10.1186/s12940-016-0145-9.

R Core Team, 2020. R: a language and environment for statistical computing.

Rich, D.Q., Liu, K., Zhang, Jinliang, Thurston, S.W., Stevens, T.P., Pan, Y., Kane, C., Weinberger, B., Ohman-Strickland, P., Woodruff, T.J., Duan, X., Assibey-Mensah, V., Zhang, Junfeng, 2015. Differences in birth weight associated with the 2008 Beijing olympics air pollution reduction: results from a natural experiment. Environ. Health Perspect. 123, 880–887. https://doi.org/10.1289/ehp.1408795.

Rodopoulou, S., Stafoggia, M., Chen, J., de Hoogh, K., Bauwelinck, M., Mehta, A.J., Klompmaker, J.O., Oftedal, B., Vienneau, D., Janssen, N.A.H., Strak, M., Andersen, Z.J., Renzi, M., Cesaroni, G., Nordheim, C.F., Bekkevold, T., Atkinson, R., Forastiere, F., Katsouyanni, K., Brunekreef, B., Samoli, E., Hoek, G., 2022. Long-term exposure to fine particle elemental components and mortality in Europe: results from six European administrative cohorts within the ELAPSE project. Sci. Total Environ. 809, 152205 https://doi.org/10.1016/j.scitotenv.2021.152205.

Shao, Y., Ma, Z., Wang, J., Bi, J., 2020. Estimating daily ground-level PM2.5 in China with random-forest-based spatiotemporal kriging. Sci. Total Environ. 740, 139761 https://doi.org/10.1016/j.scitotenv.2020.139761.

Shen, Y., de Hoogh, K., Schmitz, O., Clinton, N., Tuxen-Bettman, K., Brandt, J., Christensen, J.H., Frohn, L.M., Geels, C., Karssenberg, D., Vermeulen, R., Hoek, G., 2022. Europe-wide air pollution modeling from 2000 to 2019 using geographically weighted regression. Environ. Int. 168, 107485 https://doi.org/10.1016/j.envint.2022.107485.

Slama, R., Morgestern, V., Cyrys, J., Zutavern, A., Herbarth, O., Wichmann, H.E., Heinrich, J., 2007. Traffic-related atmospheric pollutants levels during pregnancy and offspring's term birth weight: a study relying on a land-use regression exposure model. Environ. Health Perspect. 115, 1283–1292. https://doi.org/10.1289/ehp.10047.

Stafoggia, M., Bellander, T., Bucci, S., Davoli, M., de Hoogh, K., de Donato, F., Gariazzo, C., Lyapustin, A., Michelozzi, P., Renzi, M., Scortichini, M., Shtein, A., Viegi, G., Kloog, I., Schwartz, J., 2019. Estimation of daily PM10 and PM2.5 concentrations in Italy, 2013–2015, using a spatiotemporal land-use random-forest model. Environ. Int. 124, 170–179. https://doi.org/10.1016/j.envint.2019.01.016.

Strak, M., Weinmayr, G., Rodopoulou, S., Chen, J., De Hoogh, K., Andersen, Z.J., Atkinson, R., Bauwelinck, M., Bekkevold, T., Bellander, T., Boutron-Ruault, M.C., Brandt, J., Cesaroni, G., Concin, H., Fecht, D., Forastiere, F., Gulliver, J., Hertel, O., Hoffmann, B., Hvidtfeldt, U.A., Janssen, N.A.H., Jöckel, K.H., Jørgensen, J.T., Ketzel, M., Klompmaker, J.O., Lager, A., Leander, K., Liu, S., Ljungman, P., Magnusson, P.K.E., Mehta, A.J., Nagel, G., Oftedal, B., Pershagen, G., Peters, A., Raaschou-Nielsen, O., Renzi, M., Rizzuto, D., Van Der Schouw, Y.T., Schramm, S., Severi, G., Sigsgaard, T., Sørensen, M., Stafoggia, M., Tjønneland, A., Monique Verschuren, W., Vienneau, D., Wolf, K., Katsouyanni, K., Brunekreef, B., Hoek, G., Samoli, E., 2021. Long term exposure to low level air pollution and mortality in eight European cohorts within the ELAPSE project: pooled analysis. BMJ 374, 1904. https://doi.org/10.1136/bmj.n1904.

Sun, Y., Li, X., Benmarhnia, T., Chen, J.C., Avila, C., Sacks, D.A., Chiu, V., Slezak, J., Molitor, J., Getahun, D., Wu, J., 2022a. Exposure to air pollutant mixture and gestational diabetes mellitus in Southern California: results from electronic health record data of a large pregnancy cohort. Environ. Int. 158, 106888 https://doi.org/10.1016/J.ENVINT.2021.106888.

Sun, H., Shin, Y.M., Xia, M., Ke, S., Wan, M., Yuan, L., Guo, Y., Archibald, A.T., 2022b. Spatial resolved surface ozone with urban and rural differentiation during 1990-2019: a space-time Bayesian neural network Downscaler. Environ. Sci. Technol. 56, 7337–7349. https://doi.org/10.1021/acs.est.1c04797.

Tan, S., Xie, D., Ni, C., Zhao, G., Shao, J., Chen, F., Ni, J., 2023. Spatiotemporal characteristics of air pollution in Chengdu-Chongqing urban agglomeration (CCUA) in southwest, China: 2015–2021. J. Environ. Manag. 325, 116503 https://doi.org/10.1016/j.jenvman.2022.116503.

Van Donkelaar, A., Martin, R.V., Li, C., Burnett, R.T., 2019. Regional estimates of chemical composition of fine particulate matter using a combined geo- science-statistical method with information from satellites, models, and monitors. Environ. Sci. Technol. 53, 2595–2611. https://doi.org/10.1021/acs.est.8b06392.

Van Donkelaar, A., Hammer, M.S., Bindle, L., Brauer, M., Brook, J.R., Garay, M.J., Hsu, N.C., Kalashnikova, O.V., Kahn, R.A., Lee, C., Levy, R.C., Lyapustin, A., Sayer, A.M., Martin, R.V., 2021. Monthly global estimates of fine particulate matter and their uncertainty. Environ. Sci. Technol. 55, 15287–15300. https://doi.org/10.1021/acs.est.1c05309.

Wang, M., Beelen, R., Basagana, X., Becker, T., Cesaroni, G., De Hoogh, K., Dedele, A., Declercq, C., Dimakopoulou, K., Eeftens, M., Forastiere, F., Galassi, C., Gražulevičiene, R., Hoffmann, B., Heinrich, J., Iakovides, M., Künzli, N., Korek, M., Lindley, S., Mölter, A., Mosler, G., Madsen, C., Nieuwenhuijsen, M., Phuleria, H., Pedeli, X., Raaschou-Nielsen, O., Ranzi, A., Stephanou, E., Sugiri, D., Stempfelet, M., Tsai, M.Y., Lanki, T., Udvardy, O., Varró, M.J., Wolf, K., Weinmayr, G., Yli-Tuomi, T., Hoek, G., Brunekreef, B., 2013. Evaluation of land use regression models for NO2 and particulate matter in 20 European study areas: the ESCAPE project. Environ. Sci. Technol. 47, 4357–4364. https://doi.org/10.1021/es305129t.

Wei, J., Li, Z., Lyapustin, A., Sun, L., Peng, Y., Xue, W., Su, T., Cribb, M., 2021. Reconstructing 1-km-resolution high-quality PM 2.5 data records from 2000 to 2018 in China: spatiotemporal variations and policy implications MODIS space-time extra-trees model ChinaHighPM 2.5 1 km resolution. Remote Sens. Environ. 252, 112136 https://doi.org/10.1016/j.rse.2020.112136.

Weichenthal, S., Bai, L., Hatzopoulou, M., Van Ryswyk, K., Kwong, J.C., Jerrett, M., Van Donkelaar, A., Martin, R.V., Burnett, R.T., Lu, H., Chen, H., 2017. Long-term exposure to ambient ultrafine particles and respiratory disease incidence in in Toronto, Canada: a cohort study. Environ. Heal. A Glob. Access Sci. Source 16, 64. https://doi.org/10.1186/s12940-017-0276-7.

WHO, 2021. Ambient (outdoor) air pollution [WWW Document]. https://www.who.int/news-room/fact-sheets/detail/ambient-(outdoor)-air-quality-and-health (accessed 10.19.21).

Wolf, K., Hoffmann, B., Andersen, Z.J., Atkinson, R.W., Bauwelinck, M., Bellander, T., Brandt, J., Brunekreef, B., Cesaroni, G., Chen, J., de Faire, U., de Hoogh, K., Fecht, D., Forastiere, F., Gulliver, J., Hertel, O., Hvidtfeldt, U.A., Janssen, N.A.H., Jørgensen, J.T., Katsouyanni, K., Ketzel, M., Klompmaker, J.O., Lager, A., Liu, S., MacDonald, C.J., Magnusson, P.K.E., Mehta, A.J., Nagel, G., Oftedal, B., Pedersen, N. L., Pershagen, G., Raaschou-Nielsen, O., Renzi, M., Rizzuto, D., Rodopoulou, S., Samoli, E., van der Schouw, Y.T., Schramm, S., Schwarze, P., Sigsgaard, T., Sørensen, M., Stafoggia, M., Strak, M., Tjønneland, A., Verschuren, W.M.M., Vienneau, D., Weinmayr, G., Hoek, G., Peters, A., Ljungman, P.L.S., 2021. Long-term exposure to low-level ambient air pollution and incidence of stroke and coronary heart disease: a pooled analysis of six European cohorts within the ELAPSE project. Lancet Planet. Heal. 5, e620–e632. https://doi.org/10.1016/S2542-5196(21)00195-9.

Wong, D.W., Yuan, L., Perlin, S.A., 2004. Comparison of spatial interpolation methods for the estimation of air quality data. J. Expo. Anal. Environ. Epidemiol. 14, 404–415. https://doi.org/10.1038/sj.jea.7500338.

Wu, Y., Di, B., Luo, Y., Grieneisen, M.L.M.L., Zeng, W., Zhang, S., Deng, X., Tang, Y., Shi, G., Yang, F., Zhan, Y., Yang, F., Zhan, Y., 2021. A robust approach to deriving long-term daily surface NO2 levels across China: correction to substantial estimation bias in back-extrapolation. Environ. Int. 154, 106576 https://doi.org/10.1016/j.envint.2021.106576.

Yanosky, J.D., Paciorek, C.J., Schwartz, J., Laden, F., Puett, R., Suh, H.H., 2008. Spatio-temporal modeling of chronic PM10 exposure for the Nurses' health study. Atmos. Environ. 42, 4047–4062. https://doi.org/10.1016/j.atmosenv.2008.01.044.

Ye, W.F., Ma, Z.Y., Ha, X.Z., Yang, H.C., Weng, Z.X., 2018. Spatiotemporal patterns and spatial clustering characteristics of air quality in China: a city level analysis. Ecol. Indic. 91, 523–530. https://doi.org/10.1016/j.ecolind.2018.04.007.

Zhang, Z., Wang, J., Hart, J.E., Laden, F., Zhao, C., Li, T., Zheng, P., Li, D., Ye, Z., Chen, K., 2018. National scale spatiotemporal land-use regression model for PM2.5, PM10 and NO2 concentration in China. Atmos. Environ. 192, 48–54. https://doi.org/10.1016/j.atmosenv.2018.08.046.

Zhu, Y., Hinds, W.C., Kim, S., Shen, S., Sioutas, C., 2002. Study of ultrafine particles near a major highway with heavy-duty diesel traffic. Atmos. Environ. 36, 4323–4335. https://doi.org/10.1016/S1352-2310(02)00354-0.